CONFORMAL INKJET PRINTED ANTENNAS FOR SMALL SPACECRAFT

by

Muhammadeziz Tursunniyaz

A thesis submitted in partial fulfillment
of the requirements for the degree

of

MASTER OF SCIENCE

in

Electrical Engineering

Approved:

Reyhan Baktur, Ph.D. Major Professor	Doran Baker, Ph.D. Committee Member
Chris Winstead, Ph.D. Committee Member	Mark R. McLellan, Ph.D. Vice President for Research and Dean of the School of Graduate Studies

UTAH STATE UNIVERSITY
Logan, Utah

2017

ABSTRACT

Conformal Inkjet Printed Antennas for Small Spacecraft

by

Muhammadeziz Tursunniyaz, Master of Science

Utah State University, 2017

Major Professor: Reyhan Baktur, Ph.D.
Department: Electrical and Computer Engineering

Small spacecraft such as CubeSats are becoming one of the popular space vehicles for future deep space exploration missions, scientific observations, data collection and telecommunications within the scientific and commercial sectors. UAVs are becoming multifunctional and getting smaller in size so that some of them even can fit on ones palm. Effectively using the limited surface areas of the CubeSats and UAVs is extremely important to accommodate the various surface mounted components. Inkjet printing of conformal antennas directly on the cover glass of the solar cells of the CubeSats or on the wing or other parts of UAVs is a potential solution for saving the limited real estate.

This thesis work presented a faster, better and cheaper way of inkjet printing antennas on rigid substrates such as glass or solar cells, which has a potential of integrating the antennas with the solar panel of the small spacecraft to save the limited real-estate. Several meshed and solid patch antennas printed on a space certified AF32 glass using the printing procedure outlined in this thesis and measured to verify the effectiveness of the inkjet printing procedures. A high gain reflectarray with optical transparency of 95% was inkjet printed on space certified AF32 glass and BOROFLOAT glass and measured to verify the antenna performance and solar panel efficiency. Measurement results showed that the inkjet

printed reflectarray integrated on top of the solar panel has a gain of 21.5 dB. The solar panel efficiency was dropped by around 6% due to the inkjet printed reflectarray on glass.

A simple conformal dual-band antenna for UAV application was designed with ANSYS HFSS and fabricated in the lab using a foam substrate. The measured antenna performances agreed well with the simulation results. This dual-band antenna also can be inkjet printed directly on the wing or other parts of the UAVs using the printing techniques discussed in this thesis.

(57 pages)

PUBLIC ABSTRACT

Conformal Inkjet Printed Antennas for Small Spacecraft

Muhammadeziz Tursunniyaz

Although small spacecraft are small in size and light in weight compared to the conventional satellites, they can offer lots of possibilities for space exploration, scientific observation, data collection and telecommunication. Also they cost a lot less money than the conventional satellites, and the scientific missions can be planned in a relatively short period of time by using the COTS (Commercial Off-The-Shelf) materials. However, there is a big challenge for the small spacecraft that is the limited surface area of the small spacecraft and the outnumbered components to be mounted on the surface of the small spacecraft. The most obvious one is that the competition for the limited real estate between the antenna and solar cells.

UAVs, also known as drones, have become so popular that it is not only used for military and scientific applications, but also they are available for recreational use for ordinary people. Although they are getting smaller in size so that one can put them in his pocket or on his palm, they are becoming multifunctional, which requires more sensors to be mounted on the surface of the drone to achieve its multifuncionality. For example, a recreational drone can not only take pictures and videos, but also it can transmit the picture or video in real time to the operator, which needs a camera to take the picture or videos and needs an antenna to transmit the recorded data to the operator. This requires that the limited surface area needs to be efficiently used in order to accommodate the multiple needed components. This thesis presented a faster, better and cheaper way of inkjet printing conformal antennas on the cover glass of the solar cells of the small spacecraft or on the wing or other parts of the UAV body to integrate the antenna with the solar panels of the CubeSats or with or directly printing the antenna on the UAV body to efficiently use the limited real estate.

Several meshed and solid patch antennas printed on a space certified AF32 glass substrate using the printing procedure outlined in this thesis and measured to verify the effectiveness of the inkjet printing procedures. A high gain reflectarray with optical transparency of 95% was inkjet printed on space certified AF32 glass and BOROFLOAT glass and measured to verify the antenna performance and solar panel efficiency. Measurement results showed that the inkjet printed reflectarray integrated on top of the solar panel has a gain of 21.5 dB. The solar panel efficiency was dropped by around 6% due to the inkjet printed reflectarray on glass.

A simple conformal dual-band antenna for UAV application was designed with ANSYS HFSS and fabricated in the lab using a foam substrate. The measured antenna performances agreed well with the simulation results. This dual-band antenna also can be inkjet printed directly on the wing or other parts of the UAVs using the printing techniques discussed in this thesis.

To my parents, my wife and kids

ACKNOWLEDGMENTS

I would like to express my sincere gratitude to my major professor Dr. Reyhan Baktur for her excellent guidance and generous support during my study at Utah State University. Her patience and encouragements are appreciated. She kept her office door open for me whenever I had a problem with my research projects. Whats more, she brought me into the fantastic world of electromagnetics and antennas. I also would like to thank my other committee members Dr. Doran Baker and Dr. Chris Winstead for their valuable time and effort to read my thesis and giving me the necessary support to finish my thesis.

My special thanks goes to Mr. Zakk Rhodes and Mr. Ryan Martineau from Space Dynamics Laboratory for their help with the reflectarray solar panel measurements. I also would like to thank the Wallops Flight Facility Center for their help with reflectarray measurements to verify the measurement results at Utah State University. I would like to acknowledge the help of ECE Store Coordinator Ms. Heidi Harper. She is very helpful in keeping all the lab facilities working and allowing me to use any tools or materials I needed from her store.

I would like to thank my friends in Logan who made my staying here in Logan meaningful and peaceful. Their help is appreciated.

Finally, I would like to thank my parents, brothers and sisters for their encouragement and understanding. Especially I would like to thank my father, who taught me how to stay strong in front of challenges. My wife Rizwangul is always a source of love and happiness for me. I appreciate her love and support through the years. My sons Mustafa and Mustaqim made my life colorful and full of energy. Thanks for their visiting my lab frequently to give me inspirations.

Muhammadeziz Tursunniyaz

CONTENTS

LIST OF TABLES

LIST OF FIGURES

ACRONYMS

HFSS	high frequency structure simulator
ADS	advanced design systems
UAV	unmanned aerial vehicle
DOD	drop on demand
CIJ	continuous inkjet printing
COTS	commercial off-the-shelf
CubeSat	cube satellite
PCB	printed circuit board
IC	integrated circuits
DDM	Dimatix drop manager
CAD	computer aided design
ROM	reactive organometallic ink
ISAAC	integrated solar-panel antenna array for CubeSats
ISARA	integrated solar array and reflectarray antenna
GPS	global positioning system

CHAPTER 1

INTRODUCTION

Small spacecraft is a terminology, which is not clearly defined yet. NASAs Small Spacecraft Technology Program defines it as those with a mass of less than 180 kilograms, which is one of the nine programs in the space technology mission directorate of NASA. Small spacecraft can be classified into following five categories based on their mass: (1) Minisatellite, which weighs at least 100 kG. (2) Microsatellite, which has a mass between 10 to 100 kilograms. (3) Nanosatellite, which has a mass between 1 to 10 Kilograms. (4) Picosatellite, which weighs 0.01 to 1 kilograms. (5) Femtosatellite, whose mass is less than 0.01 kilograms [1]. CubeSats, which belong to the microsatellite category, are one of the popular small spacecraft for space exploration. According to Gunters space page [2], more than 700 CubeSats have been launched into space till 2017 by universities, government agencies and space related companies around the world. Fig. 1.1 shows number of nanosatellites by announced launch years [3].

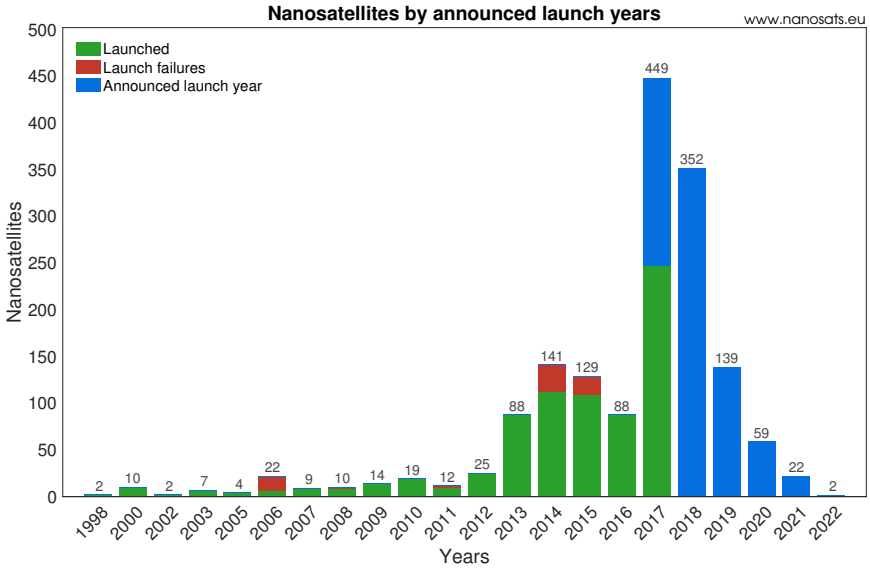

Fig. 1.1: Number of nanosatellites by announced launch years

Competition for the limited real estate between antenna and surface mounted solar cells and other electronic components is the biggest challenge for small spacecraft, especially for CubeSats [4]. Integrating the antenna with solar panel not only solve this challenge, but also it will get rid of the complex deployment mechanism, which is very costly, and reduce the payload. To minimize the risk of mission failure and increase reliability of the satellite system, integrating the antenna in a right way is very critical. Various types of antenna integration methods have been reported in the literature. Vaccaro et al. reported an integrated solar panel antenna where slot type antennas and arrays placed under the solar cells [5]. They also reported another integration method where the patch antennas placed under the solar cells [6]. A third type of integration method was reported in [7], where the optically transparent meshed patch antennas printed on top of the cover glass of the solar cells. Although the first two types of antenna integration methods were innovative, they may not be well suitable for situations where a high gain and high data rate array antenna applications needed, especially for the future deep space exploration missions. Integrating meshed patch antennas directly on top of the solar panel may allow one to integrate the high gain and highly transparent antennas on top of the solar panel, however, the antenna printing methods reported in [7] is not suitable for directly printing antennas on the cover glass of the solar cell or solar cells. This thesis work will also focus on this type of integration method and develop a novel inkjet printing procedure, which can be used to directly print antennas on the cover glass of the solar cells or directly on solar cells.

UAVs (Unmanned Aerial Vehicle) are powered, reusable aerial vehicles operated by remote control or programmed computer without on-board human pilot, which is another emerging technology in civil, defense and scientific applications. Although UAVs were not classified as small spacecraft, small in size and multifunctional UAVs are gaining more interest from defense, academia and civil application. Being small in size means limited real-estate is available for mounting antennas and other multifunctional sensors. Also for UAVs, one needs to consider the aerodynamic effects of mounted components.

Conformal antennas not only satisfy the aerodynamically requirement to reduce drag,

they also will make it possible to efficiently utilize the limited surface real estate of the small spacecraft. This will become even more obvious when the antenna of the small spacecraft is integrated with its solar cells.

Inkjet printing is a faster, better and cheaper way of printing conformal antennas on solar cells of a small spacecraft, on the wing or other parts of a UAV. An inkjet printing method with a total cost of less than $100 was reported in [8,9], where an Epson printer and conductive ink was used to inkjet print antennas on flexible transparencies. Although, this method is very cost effective, it fails to print antennas on flat rigid substrates such as glass and solar cells. The motivation for this thesis work is to develop faster, better and cheaper inkjet printing procedure to print antennas on rigid, flat surfaces such as glass and solar cells, which will provide a novel antenna integration solution for small spacecraft and UAVs, especially for CubeSats. This thesis is organized into five chapters. Chapter 1. gives an outline for the research presented in this thesis work. Chapter 2. Discusses the developed inkjet printing procedures and demonstrates some inkjet printed samples using the inkjet printing procedures developed here in this thesis. Chapter 3. discusses the inkjet printing of the Integrated Solar-Panel Antenna Array for CubeSats on a 30 cm by 20 cm glass substrate and presents the antenna and solar panel measurement results. Chapter 4. discusses the designing of a dual-band antenna for UAVs and presents the antenna measurement results. Chapter five will conclude this thesis work and outline some future works which can be done with the developed printing procedures here.

CHAPTER 2

OVERVIEW OF THE INKJET PRINTING PROCESS

2.1 Conformal Antennas

A conformal antenna is an antenna that conforms to a specific shape; The shape can be two dimensional or three dimensional in geometry. From the engineering application point, the shape can be some part of a CubeSat (Cube Satellite), UAV (Unmanned Arial Vehicle), airplane or other vehicles. The purpose of using conformal antennas is to build the antenna conformal to prescribed shape so that it becomes integrated with the structure of the specific vehicle of interest. The purpose can also be that the antenna integration makes the antenna less disturbing, less visible to the human eye. A typical additional requirement in modern defense system is that the antenna should not backscatter microwave radiation when illuminated by, for example, an enemy radar transmitter. In general, a conformal antenna conforms to a surface whose shape is determined by considerations other than electromagnetics; for example, aerodynamics or hydrodynamics [10].

2.2 Inkjet Printing

For printed electronics, including antennas, there are three well-known major fabrication techniques: (1) screen printing, (2) cleanroom fabrication, (3) inkjet printing.

Screen printing is one of the most mature printing techniques for printed electronics, which is compatible with a wide variety of functional inks and substrates. It has been utilized for decades to the fabrication of PCBs (Printed Circuit Board). For screen printing, a specially formulated ink, usually a paste, is pressed through the mask, which is a prepatterned screen, with a squeegee to form desired patterns on the substrate [11]. When the pattern is changed, the mask also needs to be modified correspondingly, which is very costly and one of the major drawbacks of screen printing. Another drawback of the screen

printing is that it is not material efficient since it is a contact printing. Considerable amount of inks remains on the screen and squeegee after the printing process [12]. This is going to be an issue especially when expensive inks such as inks containing silver particles and gold particles are used. The resolution of the screen printed patterns are limited due to the fact that high viscosity pasts are used.

Clean room based fabrication techniques such as photolithography and chemical etching are widely used as microfabrication tool for ICs (Integrated Circuit). Although it is easy to achieve relatively high precision with these fabrication techniques, they still require a prepatterned mask, which is not cost effective. Also clean rooms are expensive. Another issue concerned with the clean room based fabrication techniques is that depositing the conductive traces multiple times to overcome the skin depth will be challenging.

Compared with the conventional screen printing [13] and cleanroom fabrication techniques, inkjet printing removes the need for masks because of its direct writing ability and does not need a clean room facility, which leads to a cheaper, faster, and better way of antenna prototyping.

Inkjet printing has become an important technology for many applications, such as organic electronics [14], nanotechnology [15], tissue engineering [16], solar cells [17], batteries [18], and thin film transistors [19] on account of its ability to precisely deposit picoliter volumes of solutions or suspensions in well-defined patterns on both flexible or rigid substrates. This ability, sometimes termed as direct-write, is achieved by using computer-controlled translation stages and ink dispensers, which readily facilitates the production of complex patterns [20].

current inkjet printing technology can be categorized into two major types: DOD (Drop on Demand) and CIJ (Continuous Inkjet). In DOD method, the ink is stored in a capillary tube. The capillary tube is under negative pressure to prevent the ink from leaking. Droplets are formulated when a drop request is sent by a signal with a specific waveform. In CIJ method, a continuous stream of ink is forced to break into droplets by applying harmonic modulation. Both drop in demand inkjet printing and continuous jetting can be realized by

several ways such as piezoelectric, thermal, electrostatic and acoustic wave actuation [21]. CIJ has been successfully applied in inkjet printing, however, it requires a complicated control system compared to DOD. DOD is an efficient approach to deposit micron-scale droplets on various substrates because it is easily controlled by tuning the firing voltage and waveform, which is also compatible with various liquid solutions, especially due to its use of disposable ink reservoirs [22].

2.3 Materials and Methods

Inkjet printing of antennas on glass substrate was performed using a drop-on-demand piezoelectric material printer (DMP-2831, FUJIFILM ,Dimatix, Santa Clara, CA) [23]. The printer which was shown in Fig. 2.1, was equipped with a 16-nozzle print head (DMC-11610, Fujifilm Dimatix, Lebanon, NH, USA). The nozzles are independently controlled by inputting user defined jetting voltages and jetting waveforms. The nozzle diameter is 21.5 m with nozzle-to-nozzle spacing of 254 m. The cartridge volume of each print head is 1.5 ml. Silver nanoparticle based conductive ink JS-B40G was purchased from Novacentrix (JS-B40G, Novacentrix Corp. Austin, TX, USA). A picture of this ink was shown in Fig. 2.2. Highly transparent space certified AF-32 and BOROFLOAT glass substrates were purchased from Howard Glass [24] (Howard Glass, Worcester, MA, USA). Dielectric constant of these glass is 5.1 and the loss tangent is 0.0049 at 5 GHz. It should be noted that DMP-2831 is not the only drop-on-demand piezoelectric material printer in the market. There are many other kind of drop-on-demand piezoelectric printers such as jetlab®4 from Microfab [25]. The JS-B40 G is not the only ink which is suitable for inkjet printing as well. There are many different kinds of inks with various conductive particles and various solid content provided by different companies. Inkjet printing of custom made glucose ink with DMP-2831 is reported in [26]. The printing procedures are described in the following sessions.

2.3.1 Creating Geometry

The antenna geometry to be printed can be created in the pattern editor embedded in the Dimatix Drop Manager (DDM) software that comes with the printer. Another

Fig. 2.1: Dimatix Material Printer

Fig. 2.2: Silver ink

method, which has been found more effective, is to use an EM simulator such ANSYS HFSS, ADS Momentum, etc. to generate geometries, and then export them as dxf or other CAD (Computer Aided Design) files. After that, using ACE3000 provided by Fujifilm, a CAD file can be converted to bitmap file format that can be recognized by the DMP-

2831. The second method allows one to create more complicated patterns and to use Matlab scripting for periodic geometries. Fig. 2.3. Shows the conformal antenna geometries created in ANSYS HFSS. Some of the patterns in Fig. 2.3 were generated using the Matlab code developed in [27].

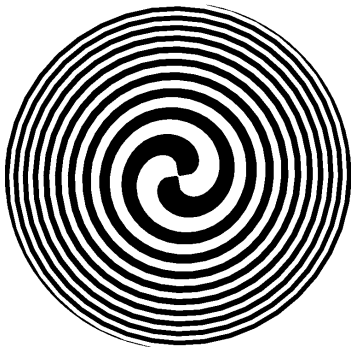

(a) Spiral antenna

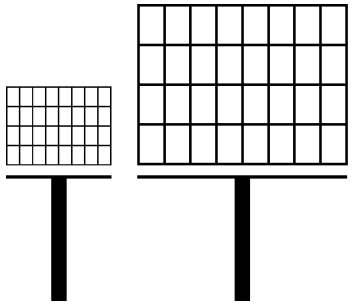

(b) Meshed patch antennas

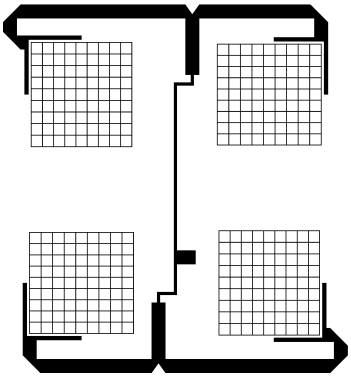

(c) Meshed patch array

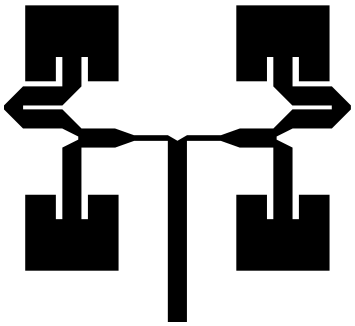

(d) Solid patch array

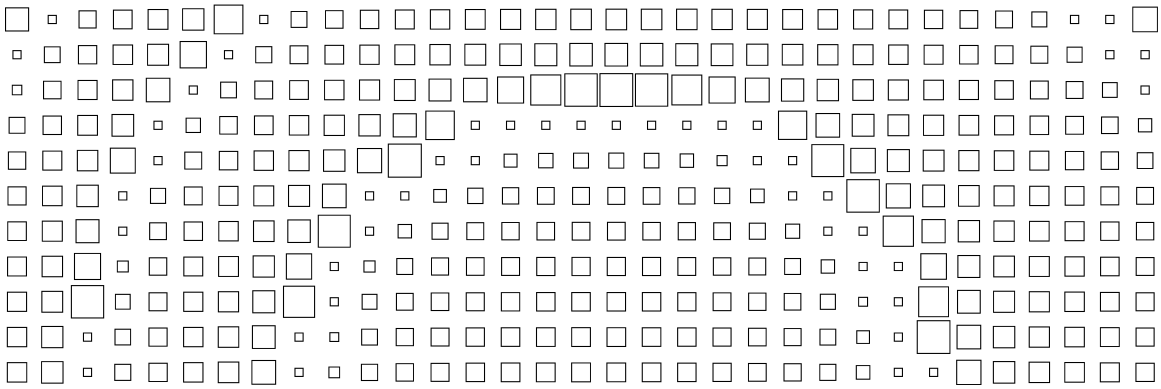

(e) Half of a reflectarray

Fig. 2.3: Conformal antenna geometries

2.3.2 Cleaning the Substrate

A clean glass surface is a prerequisite for quality printing. The substrate can be cleaned with Ethanol, Acetone, Piranha solution, oxygen plasma, nitrogen plasma or sonication [28]. In this study, the glass surface is cleaned with 75% Ethanol, which also will change the hydrophobic glass surface to hydrophilic by attaching hydroxide ion on the glass surface, resulting in an optimal wetting of the glass surface for hydrophilic inks such as Novacentrix JS-B40G [29].

2.3.3 Tuning the Nozzles

A 1 PL (Picoliter) DMC-11601 cartridge with 16 nozzles is used in this study. It is challenging to keep all the 16 nozzles jetting steadily. So it is important to tune the nozzles and choose the most stable ones while printing. Fig. 2.4 shows a drop watcher camera view of two tuned adjacent nozzles. Three to six adjacent nozzles were used in all printing processes. Custom-designed voltage waveform was applied to each nozzle to form ink droplets at controlled speed (8 0.2 m/s), frequency (5 kHz) without satellite droplets. The center-to-center distance between two adjacent printed droplets was fixed at 15m and controlled by drop spacing.The temperature of the platen and cartridge were set to 40 C.There are several parameters such as jetting voltage, jetting waveform, and drop velocity, which can be changed and optimized to get the best printing quality. In this study, a waveform provided by Novacentrix is optimized to get best printing quality, which is shown in Fig. 2.5.

2.3.4 Printing, Printing Quality, and Trouble Shooting

Before starting to print, the drop spacing, cartridge angle and drop offset need to be adjusted manually. Drop spacing is the distance between the adjacent drops. If the drop spacing is too small, then the adjacent drops will merge into one single drop, which will decrease the resolution of the printing. If the drop spacing is too large, then there will be gaps in the printed traces. The optimal drop spacing is depended on the fluid dynamics of ink and the surface properties of the substrate. The drop spacing could be optimized

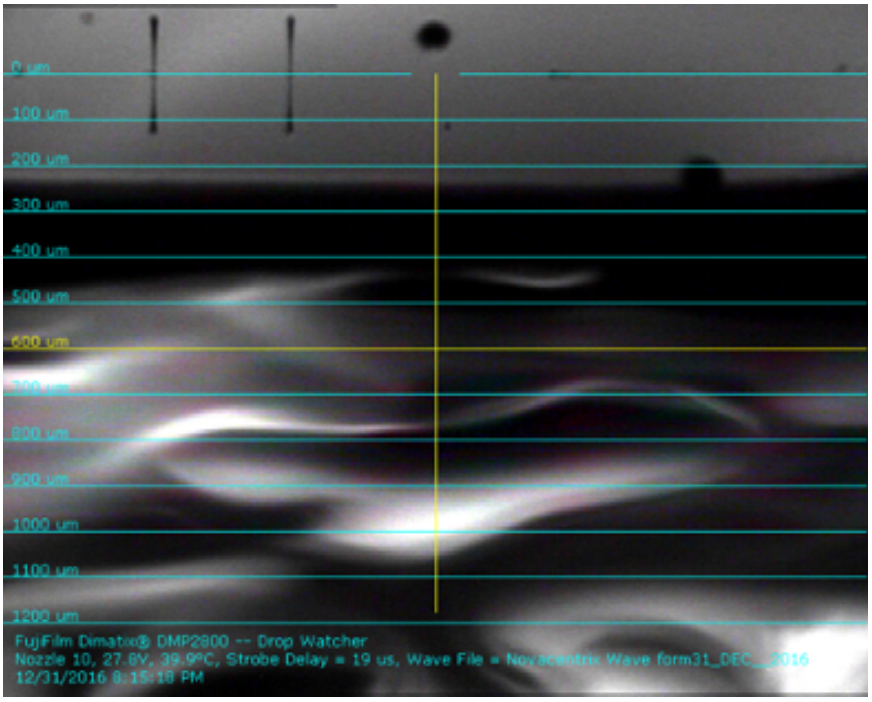

Fig. 2.4: Drop watcher camera view of tuned nozzles

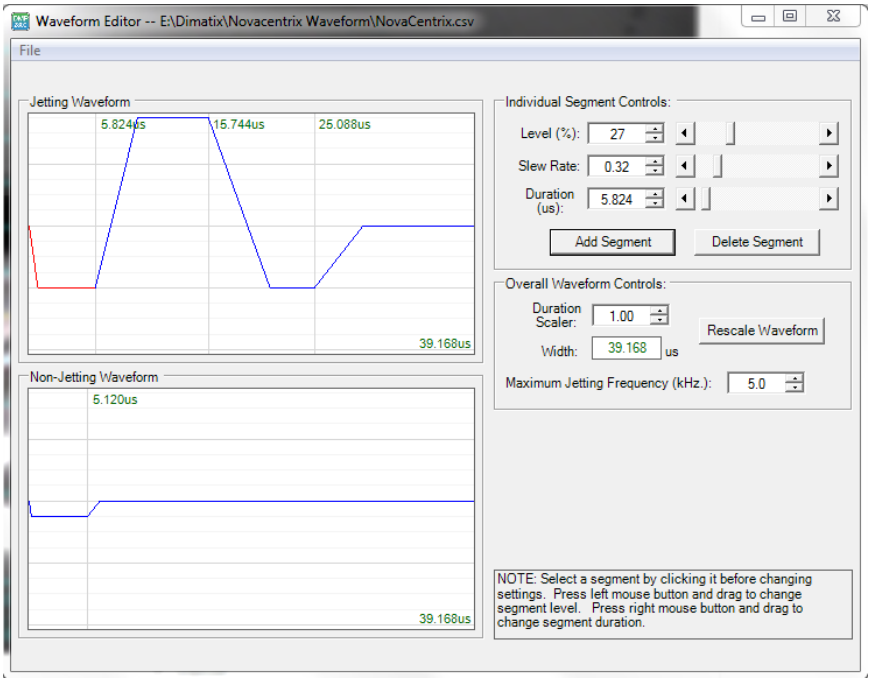

Fig. 2.5: Optimized waveform

by experimental printing. In this study, the drop spacing was set to 15 um. The cartridge angle is determined by the drop spacing and it needs to be set manually. After adjusting cartridge angle, the drop offset should be set to start the printing from the exact print origin. After the printing is done, the printed traces can be observed using the fiducial camera built in the DMP-2831 as illustrated in Fig. 2.6. Fig. 2.6 shows the difference in printing quality before and after tuning the nozzles. The drop formation can be observed by using drop watcher camera built in DMP-2831. It can be optimized by adjusting the jetting voltage and waveform.

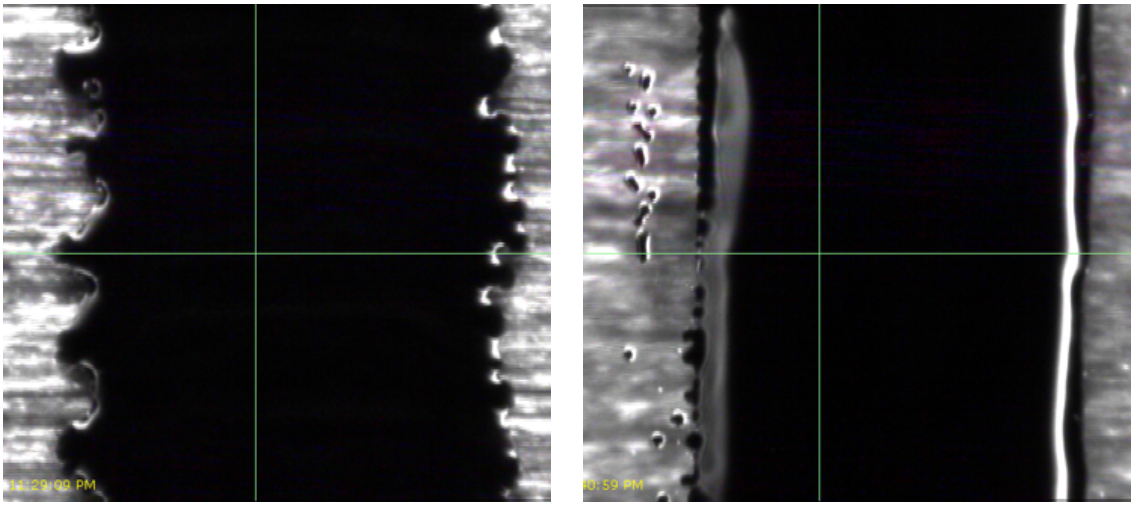

(a) Before tuning nozzles (b) After tuning nozzles

Fig. 2.6: Fiducial camera view of the feed line of a patch antenna

2.3.5 Curing

Curing is the last step for the inkjet printing process, and it can be performed in an industrial-grade oven. Controlling the curing time and temperature is crucial to achieve optimal electrical conductivity and adhesivity of the printed trace to glass surface. These two parameters are usually listed by the ink provider or can be achieved from experimentation. In this study, the printed sample are heat cured at 250 C for 10 min, which was recommended by the ink manufacturer. It should be noted that there are inks which does

not need to be heat cured such ROM (Reactive Organotmetallic) inks [30]. Fig. 2.7 shows the difference before and after curing.

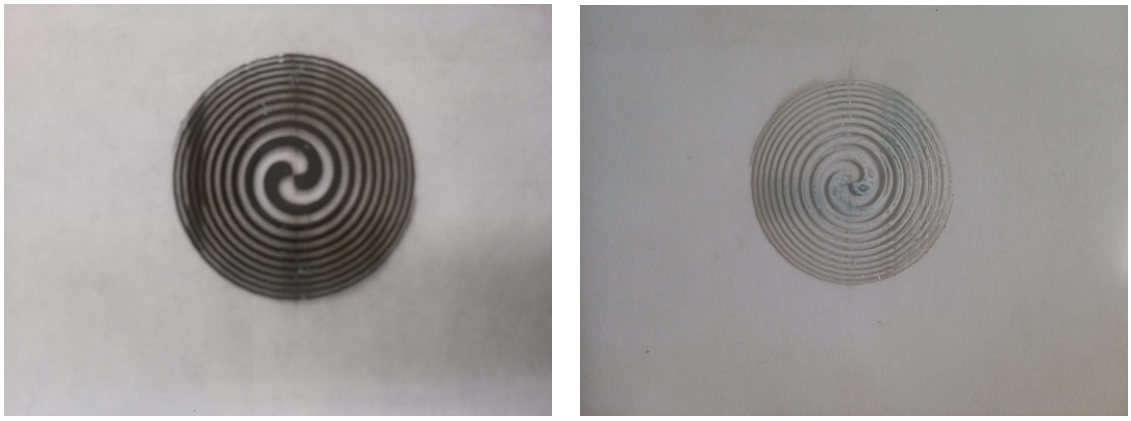

(a) Before curing (b) After curing

Fig. 2.7: Curing

2.3.6 Our Experience

With the printing procedures mentioned above, several conformal antenna patterns were printed with good printing quality, which will be discussed in detail in next chapter. With several experimental printing, it was noticed that matching the fluid dynamic properties such as contact angle, viscosity, etc. to the surface properties of the substrate is critical. It was also noticed that for the same brand of ink, the ink fluid dynamic properties vary for different lots, which requires corresponding adjustments to the waveform and the jetting voltage. However, these adjustments are very small and can be done by observing the drop formulation using drop watcher window.

The temperature of the platen and cartridge of the DMP 2831 can be controlled form room temperature to 60 °C. By setting the cartridge temperature to an appropriate value, the surface properties of the glass substrate can be changed to improve its vetting characteristics. By increasing the cartridge temperature, the viscosity of the ink can be decreased, which is an easy way for decreasing the viscosity for high viscosity inks. It was noticed that

keeping the platen and cartridge temperature the same or in close values were important to keep the drop velocity constant, which is crucial for a quality printing. If these two temperatures are set to different values, then the cartridge temperature will change towards the platen temperature while printing, which will cause the viscosity of the ink to increase or decrease. In this study, both the platen and cartridge temperatures were set to 40 C to get a quality printing.

Although relatively small patterns such as the meshed patch antennas shown in Fig. 2.3b can be printed with choosing only one nozzle in an acceptable time period, for large patterns such as the one shown in Fig. 2.3e, at least three to six nozzles should be chosen for printing to improve the printing efficiency. If only one nozzle selected for printing such large patterns, then the one nozzle could be degraded and clogged easily, which will leave some undesired gaps in the printed traces.

One of the advantages of the inkjet printing technique is that it is material efficient. With 1.5 ml volume of conductive ink, which is a nominal volume for the DMC-11601cartridge, ten to twelve pieces of half reflectarray shown in Fig. 2.3e can be printed. However, it is noticed that the nozzle plate can accumulate stray droplets in long lasted printings. When the accumulated droplets reach certain amount, they can drip onto substrate randomly, which will degrade the printing quality. In order to avoid this issue, it is suggested to clean the nozzle plate before the next printing task starts as shown in Fig. 2.8. This can be done by wiping the nozzle plate with a cleaning fabric wet with distilled water or ethanol. It should be done with extremely care to avoid any damage to the nozzles.

Storing the ink and unfinished cartridge in a right way is critical to avoid wasting ink and cartridges. The manufacturer of the JS-B40G ink suggested that the ink should be stored in the room temperature using the original cool pack to achieve maximum shelf life, but they did not provide any specific instructions for storing unfinished cartridges. Although the cartridges are disposable, it is not wise to through away unfinished cartridges especially when expensive inks such as silver or gold conductive inks are used. It was observed that the unfinished cartridge filled with JS-B40G ink was not reusable after putting the cartridge

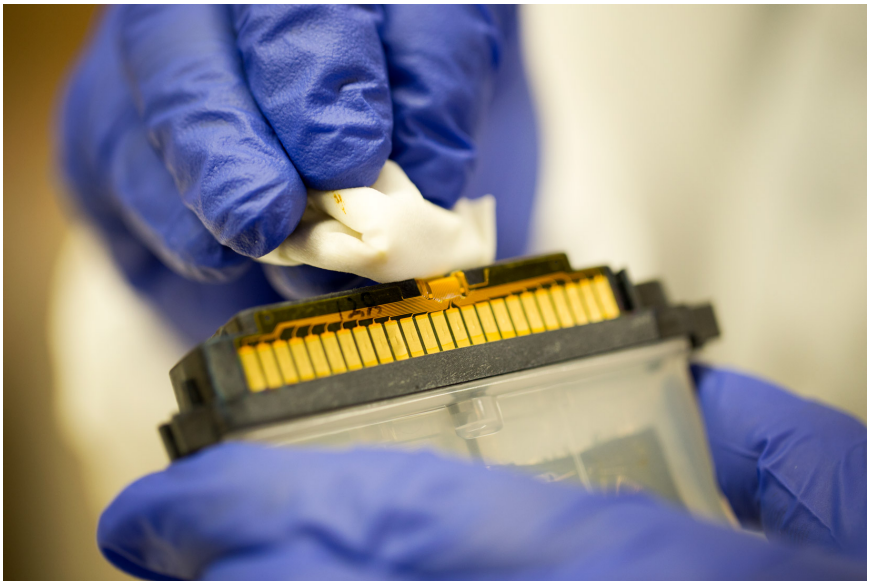

Fig. 2.8: Cleaning the nozzle plate

in the open air in four to five days. The nozzle plate was dried up and the nozzles were clogged. However, an unfinished cartridge filled with JS-B40G ink was successfully reused after storing it in the fridge for more than 30 days. It should be noted that this trick may not work with other inks. One should consult with the manufacturer of the ink to find out the best storing method or do some experiment to find out the best storing method.

2.3.7 Printed Samples

Several different planar antenna geometries have been printed on AF32 glass as examples and verifications of the effectiveness of the printing procedures outlined above. Four samples are shown in Fig. 2.9, where a spiral antenna, a 5 GHz microstrip patch and two 5 GHz meshed patch antennas with different line thickness have been printed on four pieces of glass. The detailed examination of the printed traces is shown in Fig. 2.10, Fig. 2.11 and in Fig. 2.12. The meshed patch antenna with 0.2 mm line thickness has an optical transparency of 82%, which is determined as the ratio of see-through area of the mesh over the patch area.

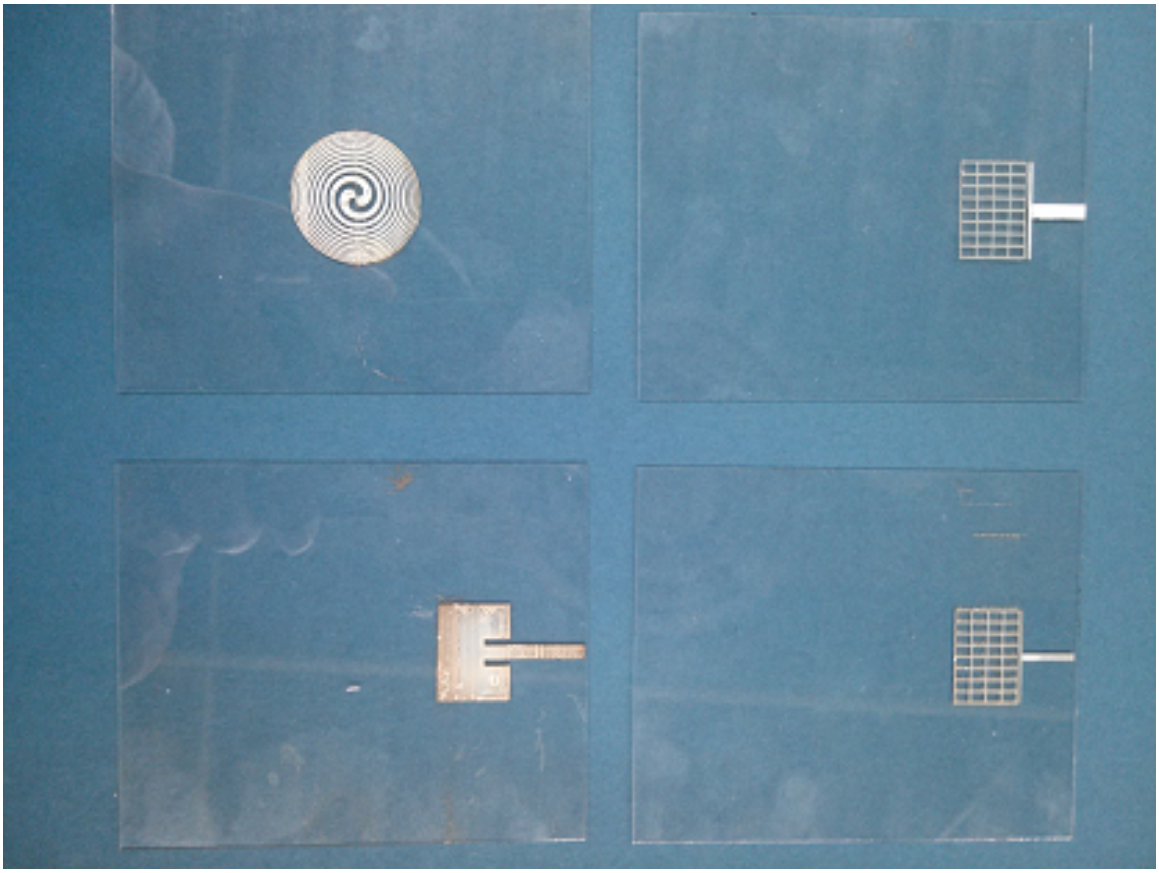

Fig. 2.9: Sample 5 GHz antennas printed on glass

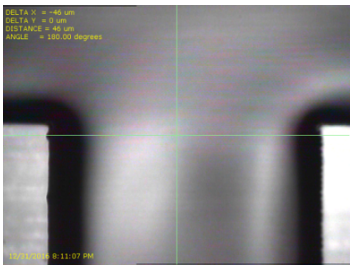

(a) Inset gap

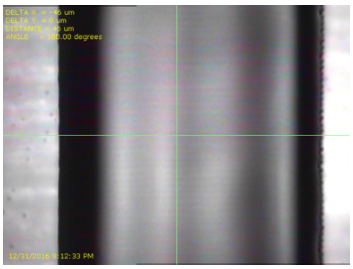

(b) Feed line

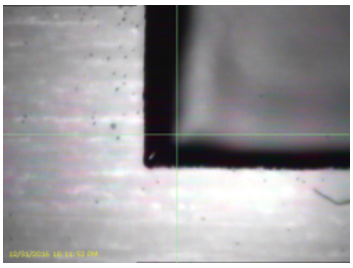

(c) Left corner of the patch

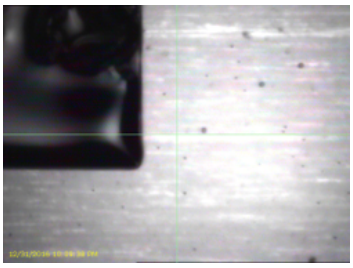

(d) Right corner of the patch

Fig. 2.10: Printing details of solid patch antenna

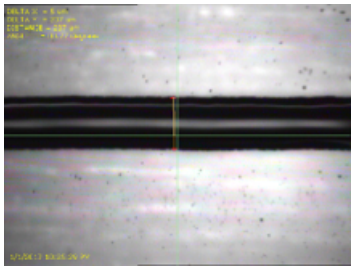

(a) 0.2 mm thick meshline

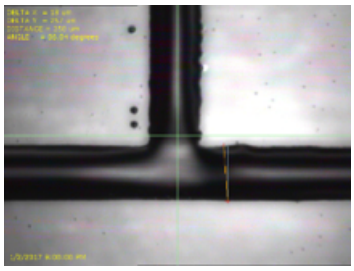

(b) Intersection of meshlines

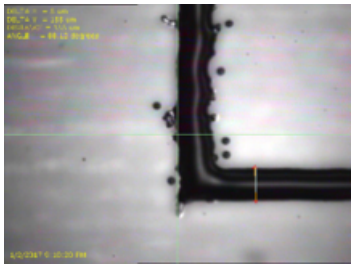

(c) 0.1 mm thick meshline

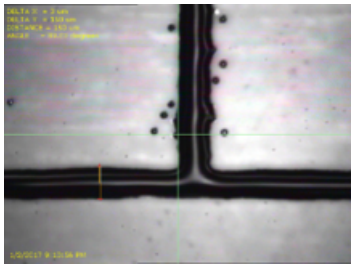

(d) Intersection of meshlines

Fig. 2.11: Printing details of meshed patch antenna

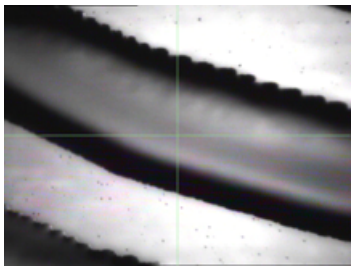

(a) Spiral arm

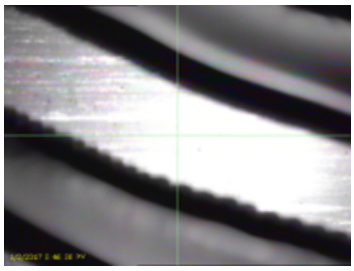

(b) Gap between spiral arms

Fig. 2.12: Printing details of spiral antenna

Fig. 2.10 showed that the printed traces have sharp and smooth edges and corners. The width of the microstrip line in Fig. 2.10b is 1.2 mm. Meshlines with different thickness was shown in Fig. 2.11. It is clear from Fig. 2.11a and Fig. 2.11b that the 0.2 mm thick meshlines have sharp and smooth edges. Although there were a few stray single droplets around the intersections of the meshlines in Fig. 2.11b, they diameter is around 5 um and not visible to bare eyes. As the line thickness decrease to 0.1 mm, the printing quality start to degrade

by accumulation of stray droplets around the edges of the meshlines as shown in Fig. 2.11c and Fig. 2.11d. From Fig. 2.12a and Fig. 2.12b, it is clearly seen that the curvature of the spiral arms are smooth and clean. The gaps between the arms are well separated. These printing details confirms the effectiveness of the printing procedures developed here. Although these printed patterns are very simple, the same printing procedures can be used for quickly prototyping of more complicated planar patterns such as reflectarrays, transmitarrays, planar lenses and other periodic structures.

The printed antennas have been measured to verify the prototyping effectiveness. All solid patch, meshed patch and reflectarray antennas have been found functioning as expected. As an example, only the S11 parameter of the 5 GHz meshed patch antenna is presented. The antenna is measured by itself (Fig. 2.13a) and then by integrated on a two-cell solar panel (Fig. 2.13b), and the results are plotted in Fig. 2.14. It is seen that solar cell introduced some loss to the antenna, as well as shifted the resonate frequency to the right. These results are consistent as predicted in the paper [31], validating the effectiveness of this fast inkjet printing method.

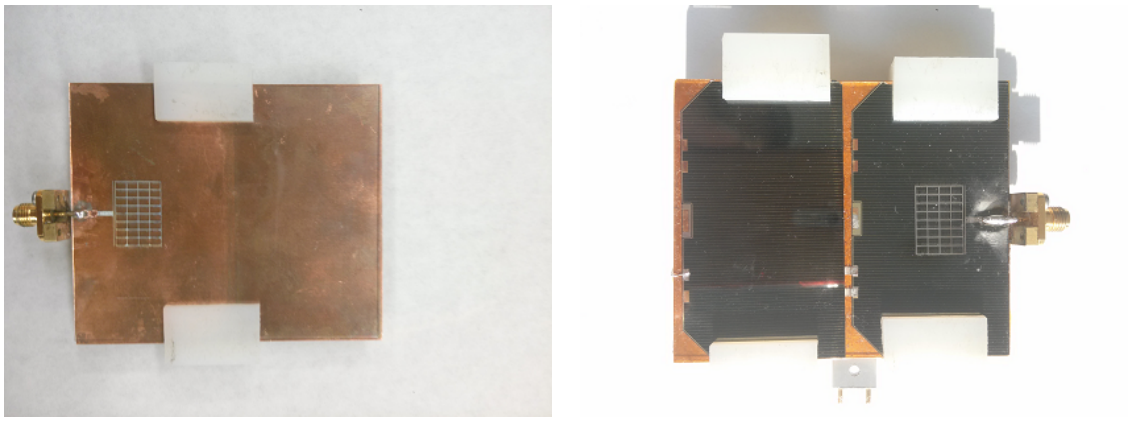

(a) Without solar cell (b) With solar cell

Fig. 2.13: 5GHz Printed antennas on test fixtures

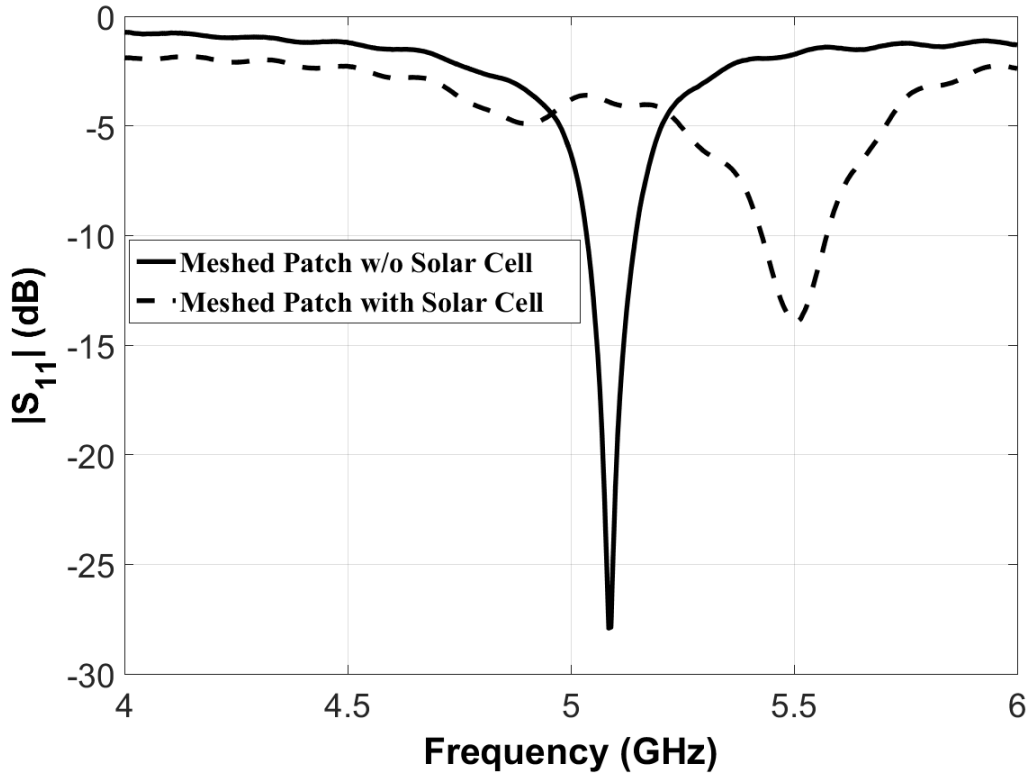

Fig. 2.14: Measured S11 of the seshed 5 GHz antenna on cover glass with and without solar cells underneath

CHAPTER 3

INKJET PRINTING OF INTEGRATED SOLAR-PANEL ANTENNA ARRAY FOR CUBSATS (ISAAC)

As CubeSat applications are calling for faster and bigger data transmission, a paradox on the antenna design is inevitable, where an antenna with high gain and data rate requires larger size that challenges CubeSat's payload. NASA's ISARA is a great solution to resolve such problem as it integrated a reflectarray antenna under the solar panel [32]. But ISARA is not applicable when the sun and the communication front-end are required to be on the same direction. This project presents an alternative design where a highly transparent reflectarray antenna is directly printed on top of solar cells. As the antenna is integrated on top of solar cells, it does not require additional space or deployment mechanism. Such an integration provides a conformal, low cost, highly efficient, and low risk antenna design that enables big data transmission.

This project is a collaborative effort that includes Utah State University, Space Dynamics Laboratory, NASA Goddard Space Flight Center, and Wallops Flight Facility. Both the solar panel and antenna use only space certified materials and modular design.

An X-band reflectarray reported in [33] was inkjet printed both on space certified AF32 glass and BOROFLOAT [34] glass using the printing procedures outlined in Chapter 2. Fig. 3.1 shows this inkjet printed X-band reflectarray with square loops as unit cells printed on a piece of 30 cm by 20 cm glass, which is then to be assembled on a solar panel. For both the meshed patch antenna in Fig. 2.3b and the reflectarray, it is possible to improve the optical transparency; however, one may sacrifice the antenna properties, and therefore a reasonable trade off has to be considered. Each trace has been printed multiple times to ensure the thickness of the conductive ink layer is sufficiently larger than the microwave skin depth. The precision in printing multiple times has been very good and the time used to print those antennas are much shorter than screen printing. For example, the reflectarray

in Fig. 3.1 was printed within 12 hours.

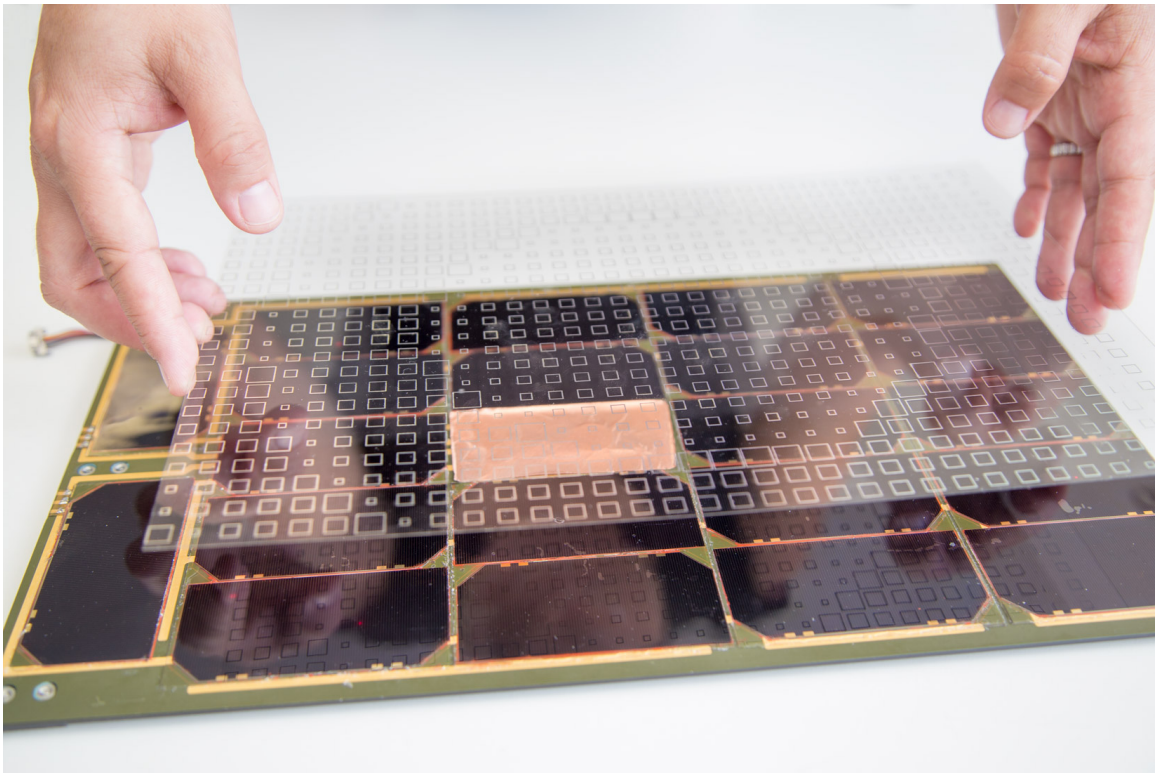

Fig. 3.1: Printed reflectarray on test fixtures

3.1 Considerations of the Substrate

The main challenge is to choose a suitable glass to print the reflectarray on. The substrate needs to provide a minimal thickness to provide minimum needed phase range for the antenna, and sufficient transparency. At this time, we have chosen a Schott Borofloat Glass from Howardglass to print the initial design on. The properties of the glass are as follows. Optical transparency is around 92.5%, thickness is 2.75 mm, dielectric constant is 4.6 (25 C°, 1 MHz), and the loss tangent is 37 x 10-4 (25 C° , 1 MHz). The glass still has a potential issue for a future mission because it is thick and the blackening issue may not be avoidable. Hence, our team is in search of an alternative cover glass material such as acrylics for the next prototype.

3.2 Inkjet Printing

The reflectarray was inkjet printed with DMP-2831 and Novacentrix JS-B40G ink from Novacentrix using the same procedures outlined in Chapter 2. The printed traces of the reflectarray on Borofloat glass was examined with the fiducial camera and it found to be the same as with the printing quality on AF-32 glass, which verified the effectiveness of the printing procedures. With optimally tuned 6 consecutive nozzles, the reflectarray was printed within six hours, which implies the importance of tuning nozzles. The inkjet printed reflectarray on glass was heat cured in an industrial oven at 250 C° for 10 minutes to burn off nonconductive components to get better conductivity.

3.3 Coating

Given the fact that the printed reflectarray must be capable of being handled under normal working conditions such as touching and minor scratching, the printed glass was coated with Parylene HT, a fluorinated variant of the basic di-para-xylene. Parylene is applied by vapor deposition of the reactive monomer. Parylene HT has a very low coefficient of friction and capable of withstanding temperatures up to 450 C°. It was applied to a thickness of 0.5 mil to 1 mil. Coating was done at Wallops Flight Facility.

3.4 Reflectarray Measurement Results

The measurements have been performed on the antenna (gain, efficiency) with or without solar panel underneath, and on the solar panel with or without the antenna on top. The antenna tests were performed at Utah State University and at Wallops Flight Facility for verification. The solar panel tests were performed at the Space Dynamics Laboratory.

3.4.1 Antenna Measurements

The printed antennas were measured at USU with and without a 6U solar panel underneath. When there is no solar panel under the antenna, a copper or aluminum ground layer were added under the glass. Fig. 3.1 shows how the printed reflectarray was assembled on the solar panel. For these tests, in order to reuse the antenna and solar panel, no

adhesive is used to bond the glass and solar panel. Fig. 3.2 shows the measurement setup at USU. Fig. 3.3 and Fig. 3.4 were provided by Wallops Flight Facility when the antenna was shipped there for further measurements. USU and Wallops measurement results match well and are summarized in Table 3.1. The reference antenna in Table 3.1 was fabricated with FR4 board, which has similar electrical properties with the AF32 glass, using conventional PCB technology. The reference antenna is shown in Fig 3.5.

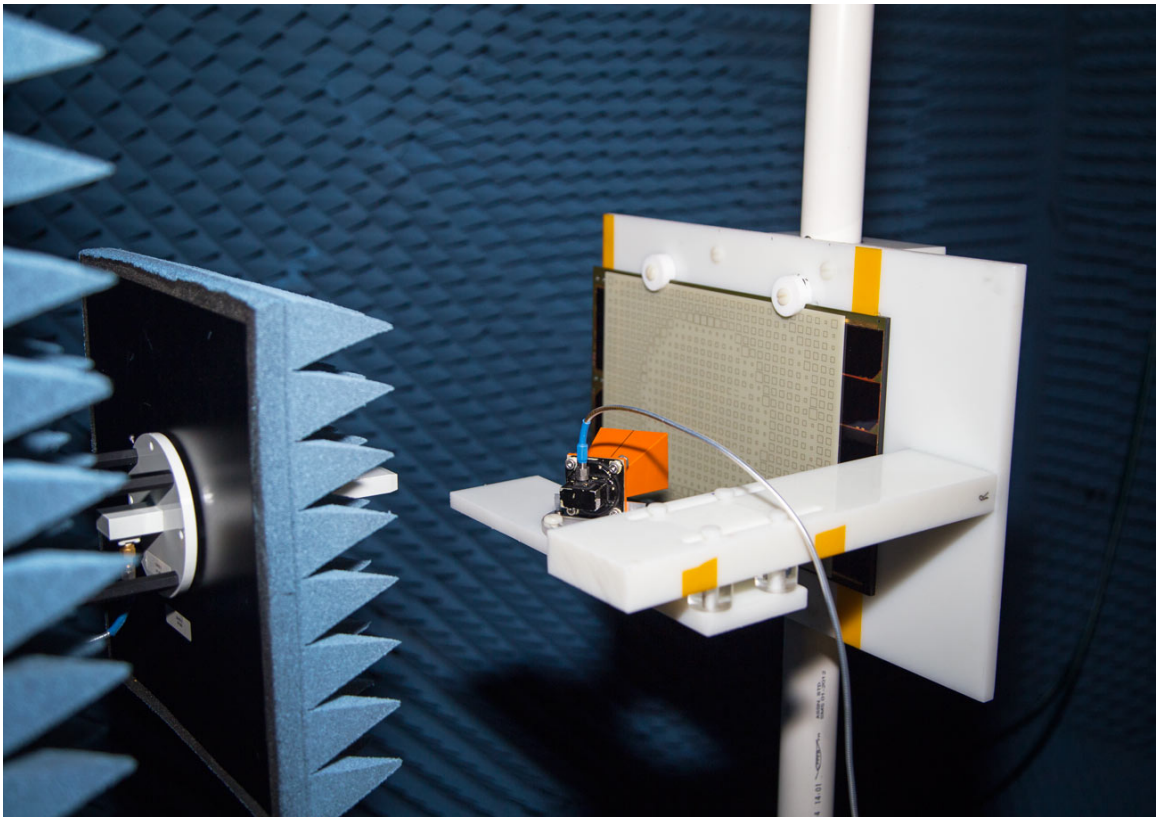

Fig. 3.2: Reflectarray measurement setup at USU

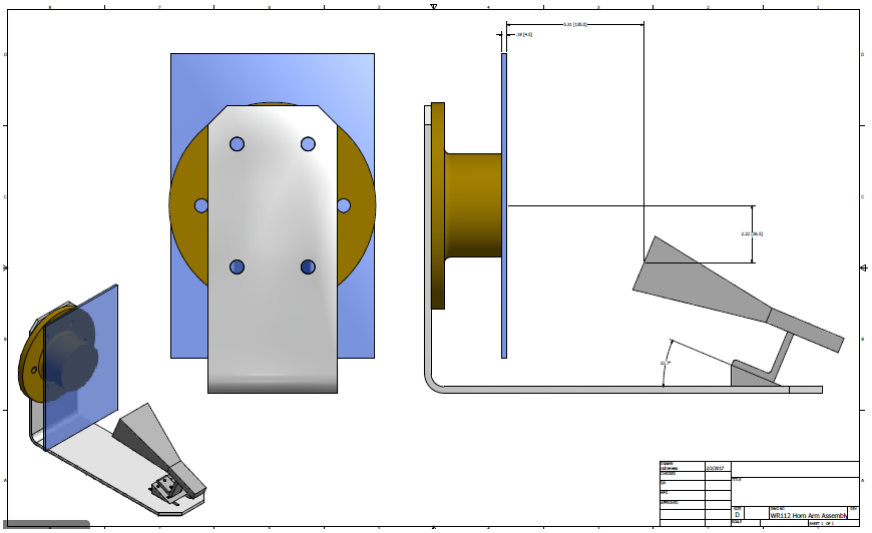

Fig. 3.3: Reflectarray measurement setup schematic at Wallops

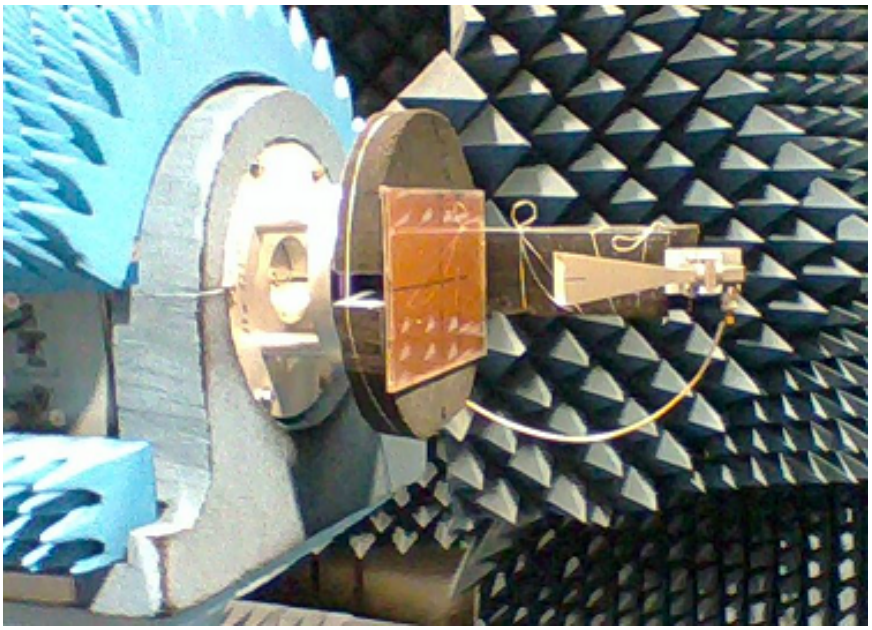

Fig. 3.4: Reflectarray measurement setup at Wallops

Table 3.1: Performance of inkjet printed reflectarray.

Reflectarray	Gain (dB)
Simulation	24.14
Reference antenna	24
Reference antenna on solar panel	22.46
Glass reflectarray	23
Glass reflectarray on solar panel	21.5

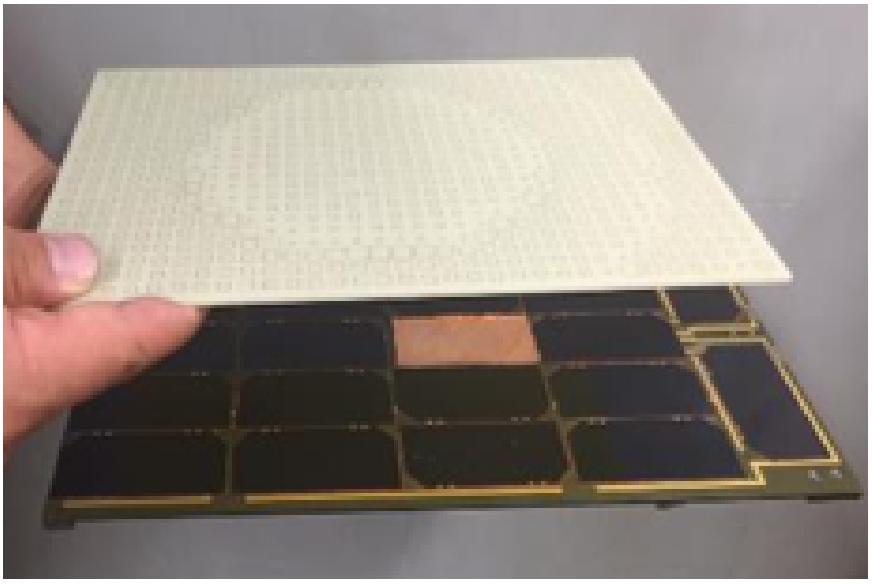

Fig. 3.5: Reference antenna

3.4.2 Solar Panel Measurements

Solar panel tests were performed using a 3U solar panel and half of the reflectarray printed on glass with a size of 10 cm by 30 cm (Fig. 3.6). The reason for this arrangement is that by the time of I-V curve measurements, a fully functional 6 U solar panel was not available. Hence, we scaled the problem to a 3U. As the reflectarray is symmetric, cutting it to half does not change its transparency. These tests were performed at the Space Dynamics Laboratory and the tests are as follows. The first test is to measure the I-V and P-V curve of a 3U solar panel. The second test is to repeat the solar panel measurements when placing a clear Schott Borofloat Glass of 10 cm by 30 cm. In the third test, the glass that goes on top of the solar panel has half of the reflectarray printed on it. The measured results are shown in Fig. 3.7 and Fig. 3.8. The efficiency of the solar panel under those three tests were then calculated and listed in Table 3.2.

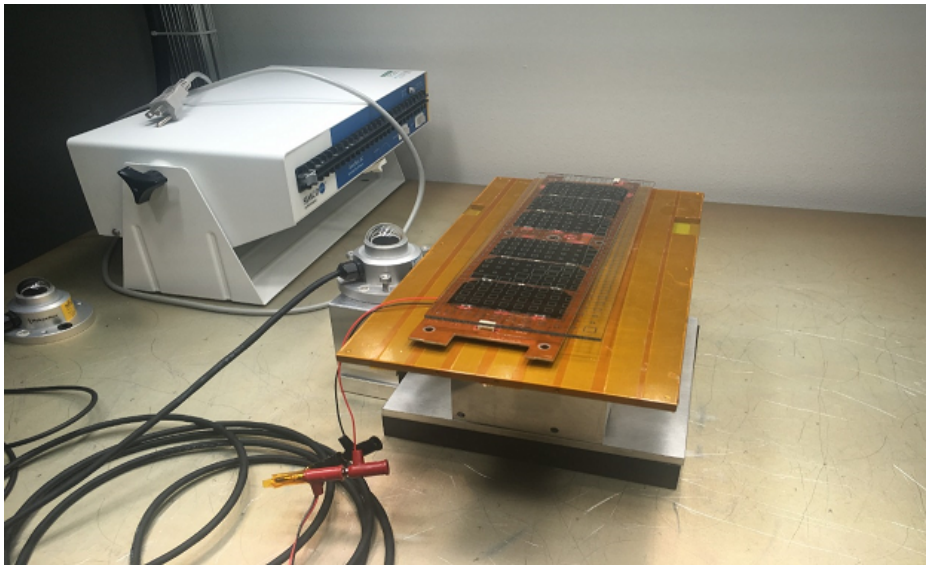

Fig. 3.6: I-V Curve Measurement Set up

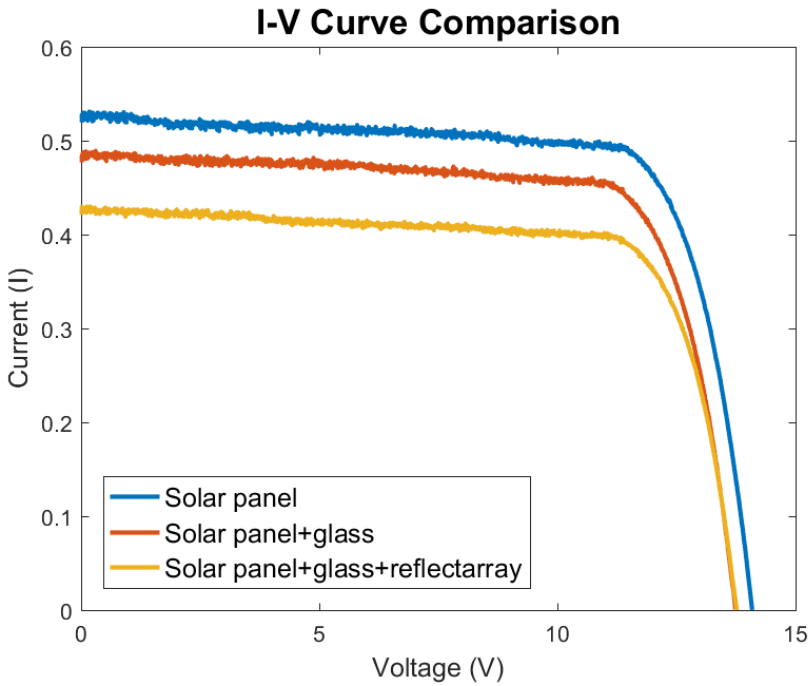

Fig. 3.7: I-V Curve Comparison

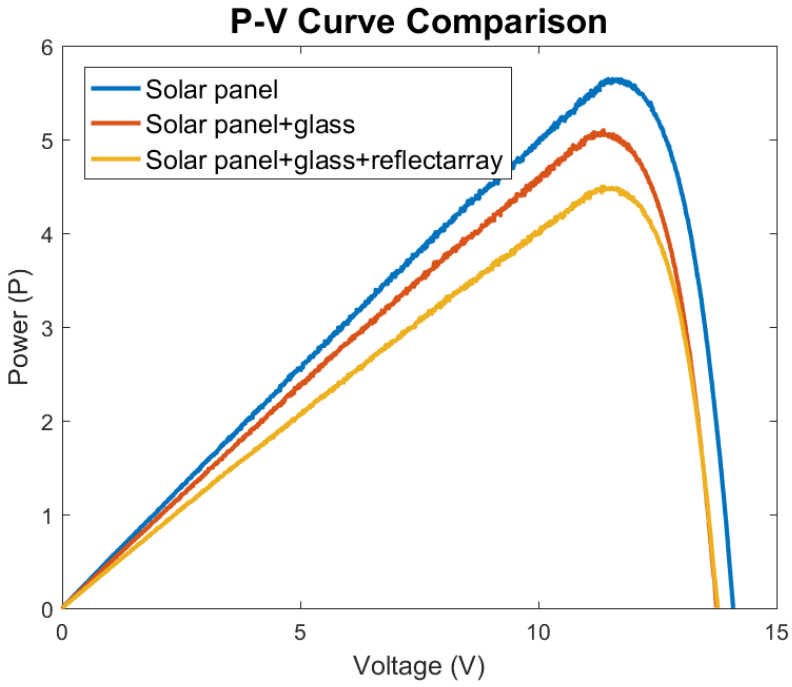

Fig. 3.8: P-V Curve Comparison

Table 3.2: Solar Panel Efficiency

Test set-up	Efficiency (%)
Solar Panel	26.1
Solar Panel with Clear Glass on Top	24
Solar Panel with Reflectarray (printed on glass) on Top	20.8

It is seen that the efficiency of the solar panel reduces to about the 90% of when it is not covered with the Schott Borofloat Glass. This is consistent with the transparency of the glass, which is about 92%. The reflectarray itself, however, reduces the efficiency of the solar panel to 88% of when it is covered with the clear glass. This reduction is higher than expected because the transparency of the reflectarray is 95%. The reasons for the lower efficiency of the solar panel under the printed reflectarray are as follows: (1) From Fig. 3.6, the 3U panel is smaller than the glass, hence the actual transparency of the printed antenna is lower than 95%, and (2) the shadows of the traces of the antenna may be higher than the dimension of the antenna elements, hence more blockage on the solar cells.

CHAPTER 4

CONFORMAL DUAL-BAND ANTENNAS FOR UAVS

4.1 About UAVs

Unmanned Aerial Vehicles (UAVs), also known as drones, have not only been used in modern warfare for attacking enemy target, intelligence, reconnaissance, surveillance and performing risky missions in unknown or dangerous environments to avoid the loss of lives [35], but also they have been widely used in civil applications such as precision agriculture [36], photogrammetry and remote sensing [37], disaster research and management [38] due to its lightweight, low cost and the ability to provide real-time fine spatial data compared to conventional satellites.

4.2 Antennas for UAVs

Antennas are one of the core communication components for the UAVs. Modern UAVs require multiple antennas for various applications such as Global Positioning System (GPS) navigation, remote control, data transmission etc. However, the real-estate suitable for antenna installation is limited for UAVs. Conformal antennas can be easily integrated into the body of the UAVs without disturbing its aero dynamical properties, which is not possible for conventional protruding antennas such as dipole or helical antennas. Dual-band antennas can reduce the number of the antennas while keeping the multifunctional capability of the antenna system of the UAVs. A conformal dual-band antenna will be a promising solution for exploiting the surface of the UAVs where the conventional antennas were usually avoided for mounting and reducing the number of antennas.

The objective of this project is to design a conformal dual-band antenna with operating frequencies f_l=2.35 GHz , f_u=5.55 GHz and f_r=2.36, where f_l is the lower resonance frequency, f_u is the upper resonance frequency and f_r is defined as the ratio of f_u to f_l, and

quickly prototype this antenna with a foam substrate and copper foil in the lab to confirm its performance.

4.3 Conformal Dual-Band Antennas

Dual-band antennas have been widely utilized in communication systems. The basic idea to design a dual-band antenna is to create a radiation mechanism which can radiate efficiently in two well separated frequency bands with expected radiation characteristics. A dual-band slot-loaded patch antenna was reported in [39]. While this antenna is dual-band and conformal, the f_r can only be changed between 1.6 to 2, which is less than 2.36. A reconfigurable slot antenna with wide tunability range was reported in [40]. Although this antenna is also conformal and f_r can be changed between 1.3 to 2.67, it needs lumped elements and extra bias network for tuning, which complicates the antenna prototyping. Since the final goal of this project is to be able to print the antennas directly on the wing or other parts of the UAV, a conformal dual-band antenna is proposed. The design procedures of this antenna will be discussed in next.

4.4 Antenna Design

The given frequency bands for the dual band antenna are 2.2002.500 GHz and 5.2505.850 GHz. Thus f_l=2.350 GHz was chosen as the center frequency for the lower frequency band and f_u =5.550 GHz for the higher frequency band. The radiation at the higher resonance frequency f_u was realized by microstrip feed patch antenna and the radiation at the lower resonance frequency f_l was realized by a square ring slot antenna, which was located on the ground plane of the patch antenna and fed by the microstrip line of the patch antenna. A copper plane was put under the ground plane of the patch antenna to reflect the back ward radiated power from the square ring slot antenna and the leaked radiation by the slot from the patch antenna.

The dual-band antenna was simulated in HFSS using Rohacell HF provided by EVONIK [41], which is a foam material with dielectric constant of 1.075 and loss tangent of 0.0002, as a substrate.The dual band antenna with the Rohacell HF substrate was quickly prototyped

in the lab by hand and measured with a Keysight N5225A Network analyzer to verify its performance. The radiation pattern and gain was measured in the NSI nearfield chamber.

4.5 Dual-band antenna with Rohacell HF Substrate

The proposed dual band antenna geometry was shown in the Fig. 4.1. The optimized antenna parameters were listed in Table 4.1. Fabricated antennas with the Rohacell HF substrate was shown in Fig. 4.2. Simulated and measured reflection coefficient results were shown in Fig.4.3. Simulated and measured E-plane and H-plane patterns for corresponding frequencies were shown in Fig. 4.4, Fig. 4.5, Fig. 4.6, and in Fig. 4.7. The simulated and measured gain of the dual-band antenna was summarized in Table. 4.2.

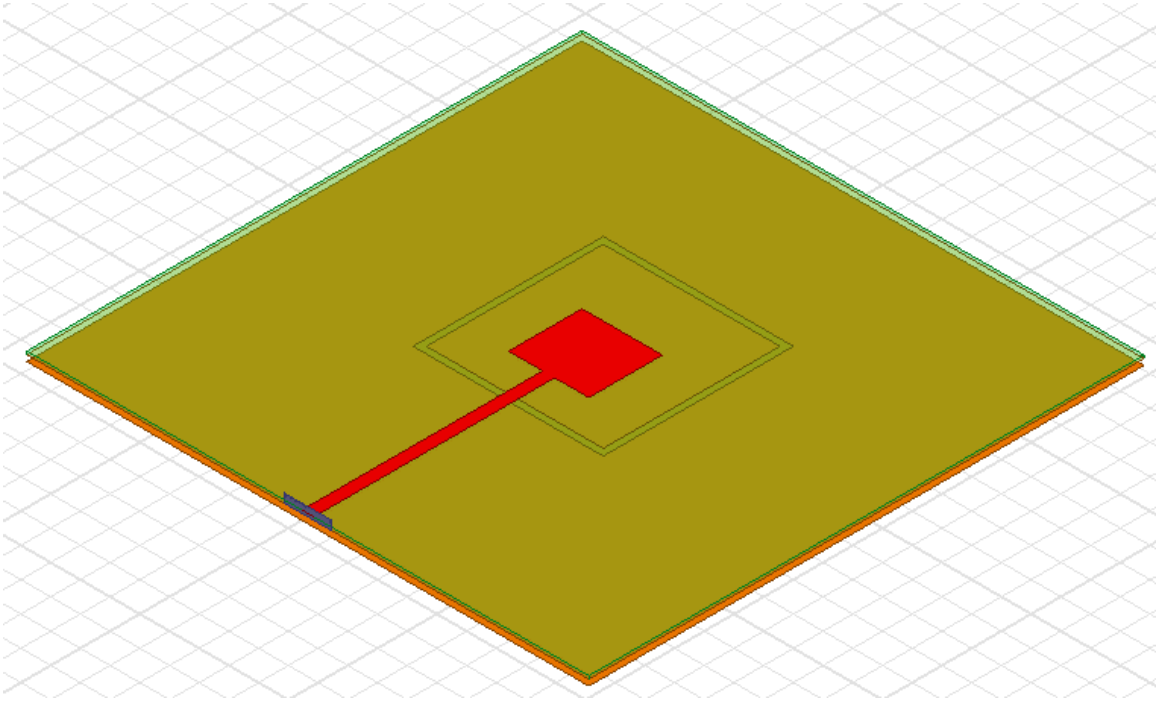

Fig. 4.1: Geometry of the dual Band antenna

Table 4.1: Optimized Antenna Parameters

Parameter	Value (mm)
L_p (Length of Patch)	24.7
W_p (Width of Patch)	27
L_{sub} (Length of Substrate)	186.85
W_{sub} (Width of Substrate)	189.15
h (Thickness of Substrate)	1
h_{copper} (Distance from ground plane to copper plane)	2
W50 (Width of 50 Ω microstrip line)	4
L_{slot} (Outer side of the square ring slot)	64
w (Width of slot)	2.25

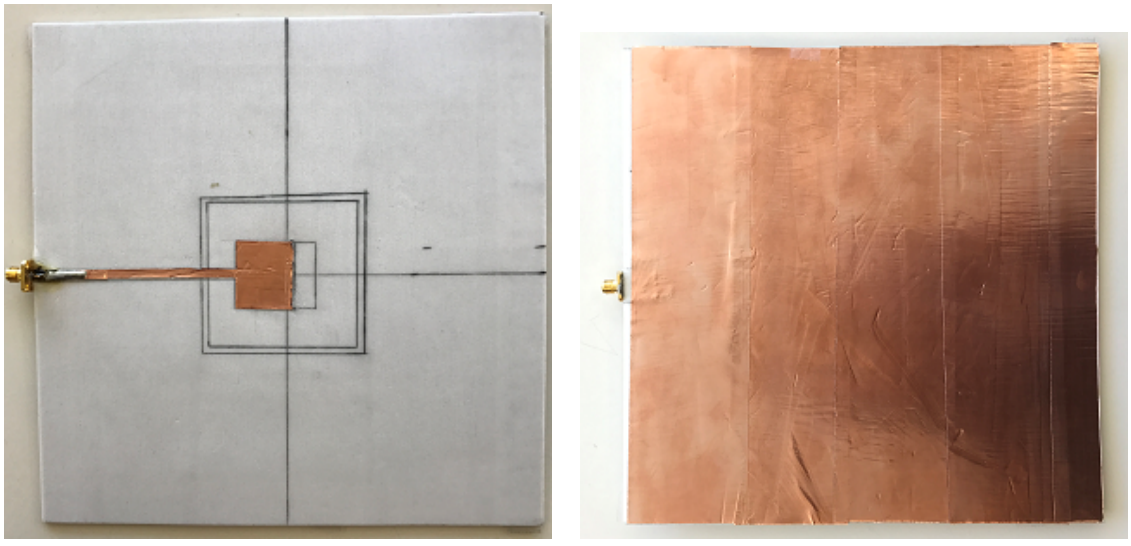

(a) Front view (b) Back view

Fig. 4.2: Fabricated dual-band antenna with Rohacell HF

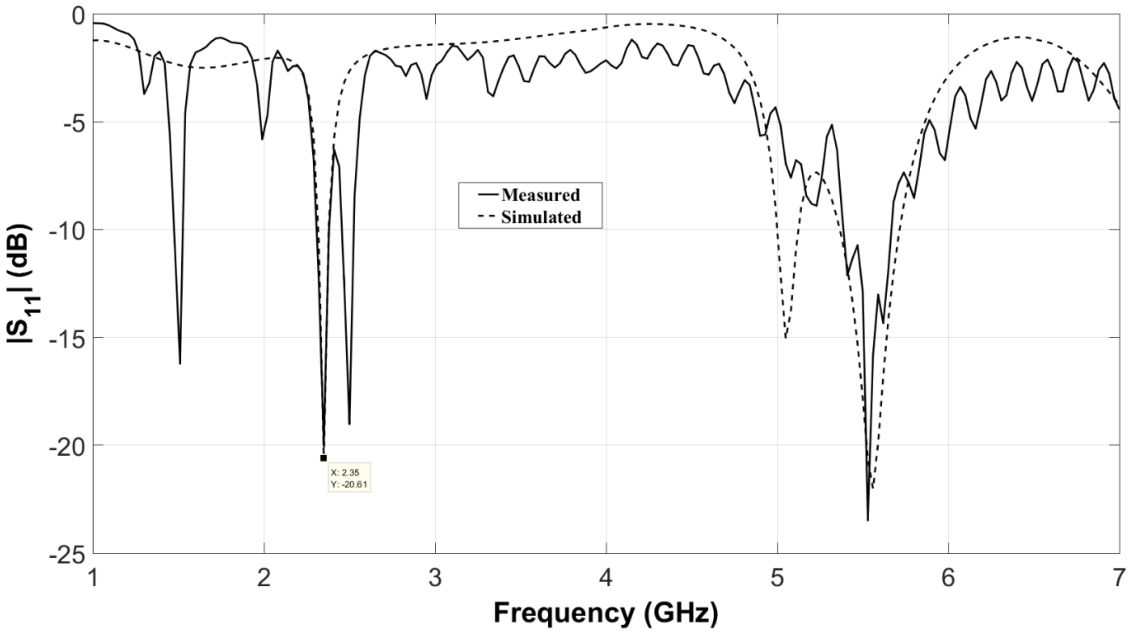

Fig. 4.3: S11 of the dual-band antenna fabricated with Rohacell HF

Table 4.2: Dual-band Antenna Performance

Frequency (GHz)	Simulated Gain (dB)	Measured Gain (dB)
2.35	7.01	7.06
5.55	5.47	5.4

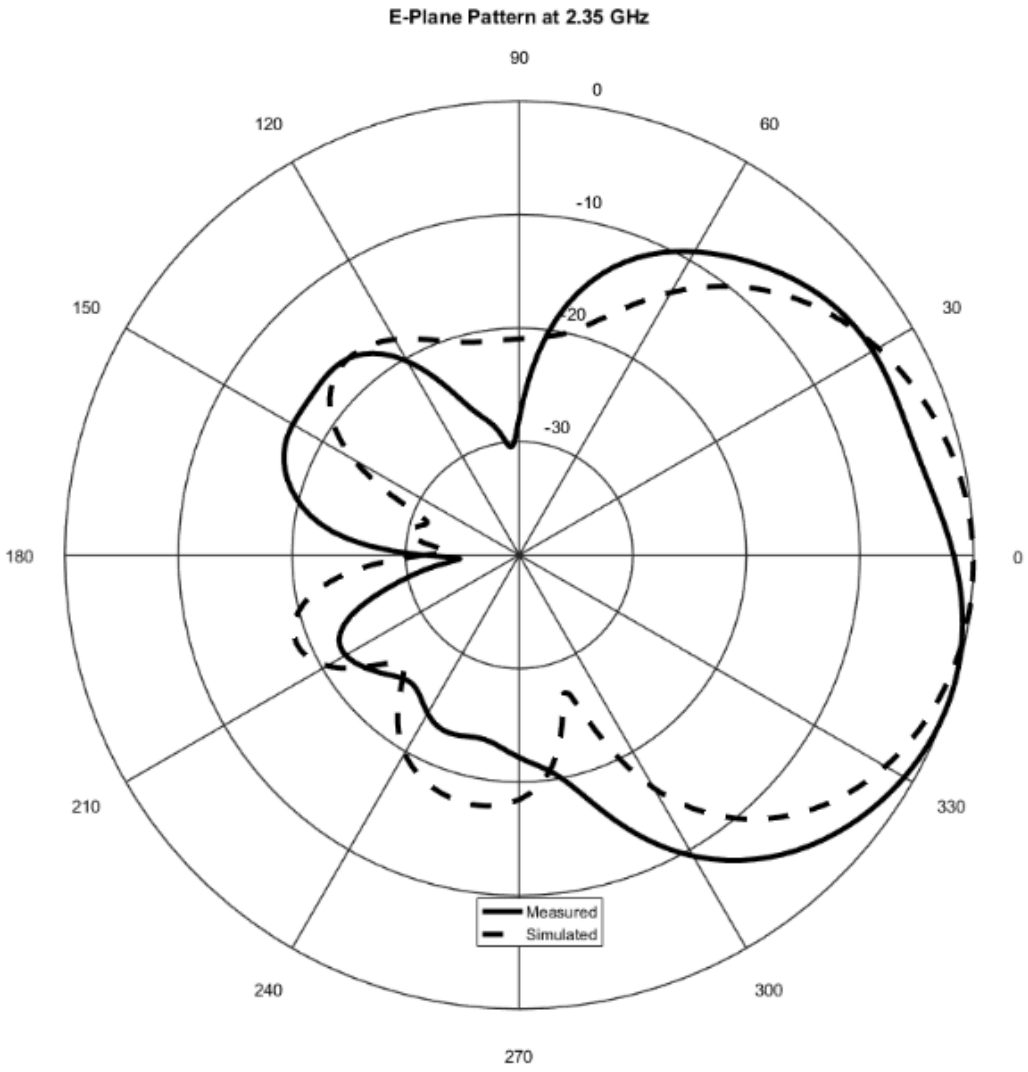

Fig. 4.4: E-Plane Radiation Pattern @2.35 GHz

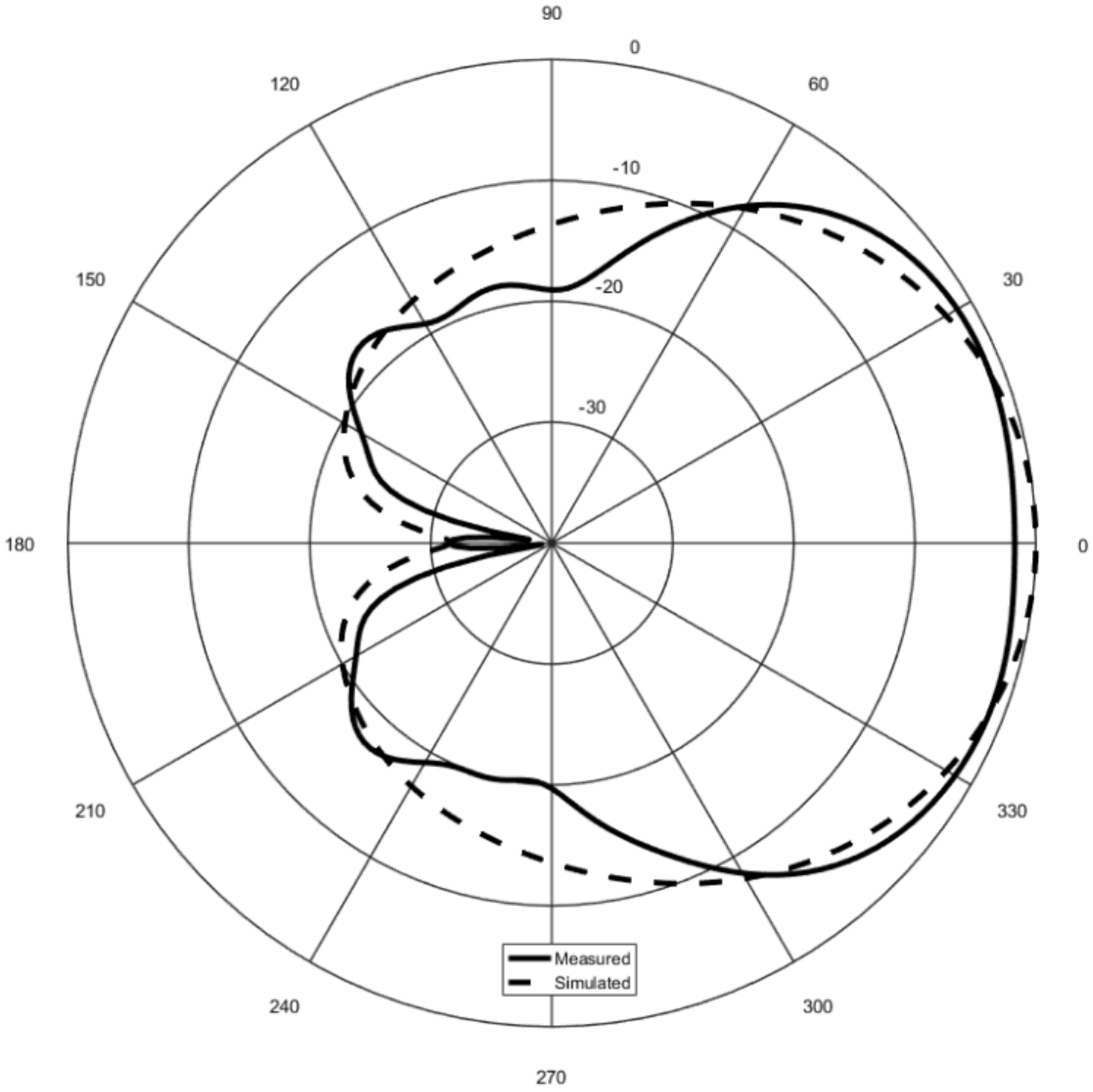

Fig. 4.5: H-Plane Radiation Pattern @2.35 GHz

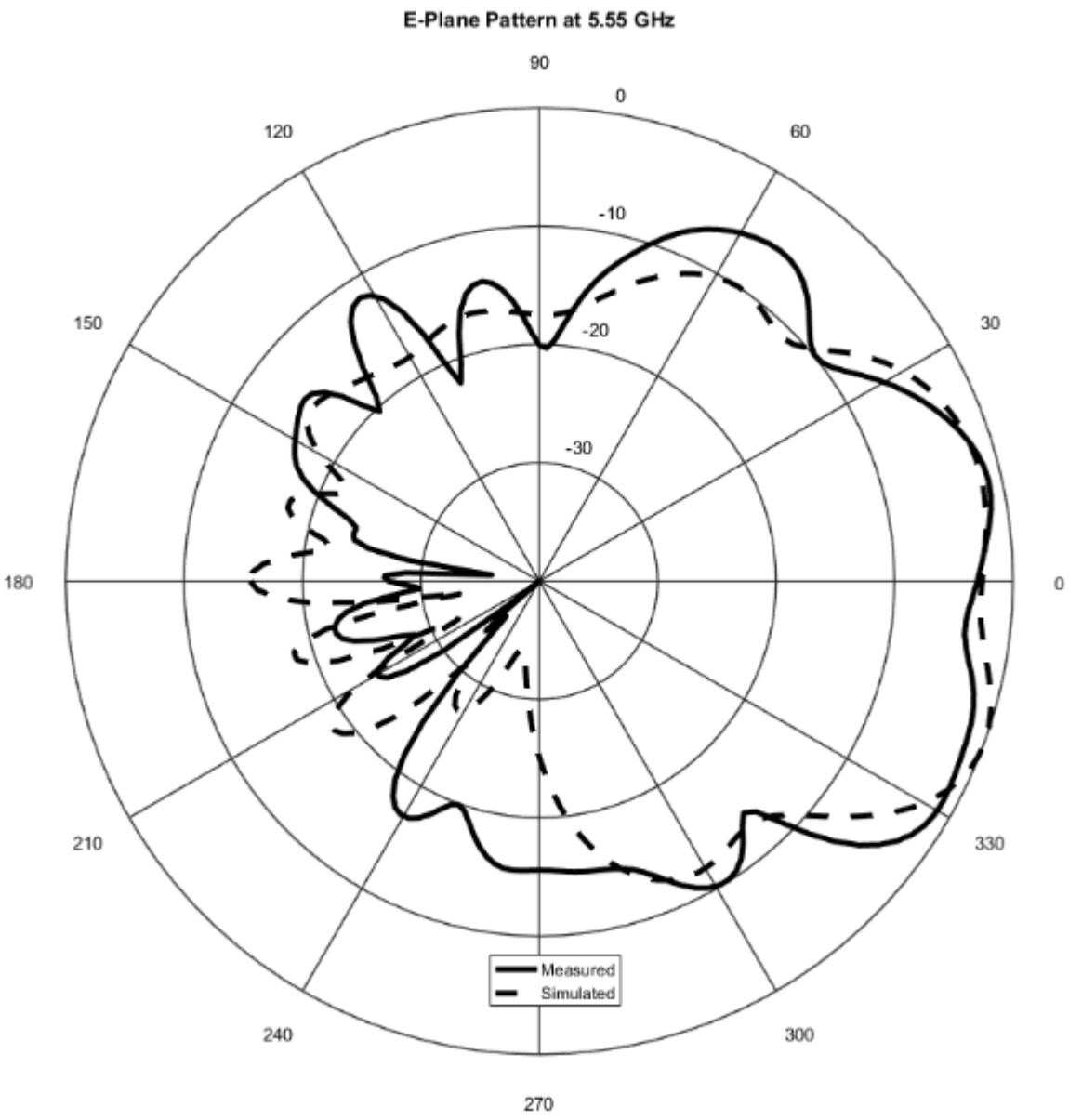

Fig. 4.6: E-Plane Radiation Pattern @5.55 GHz

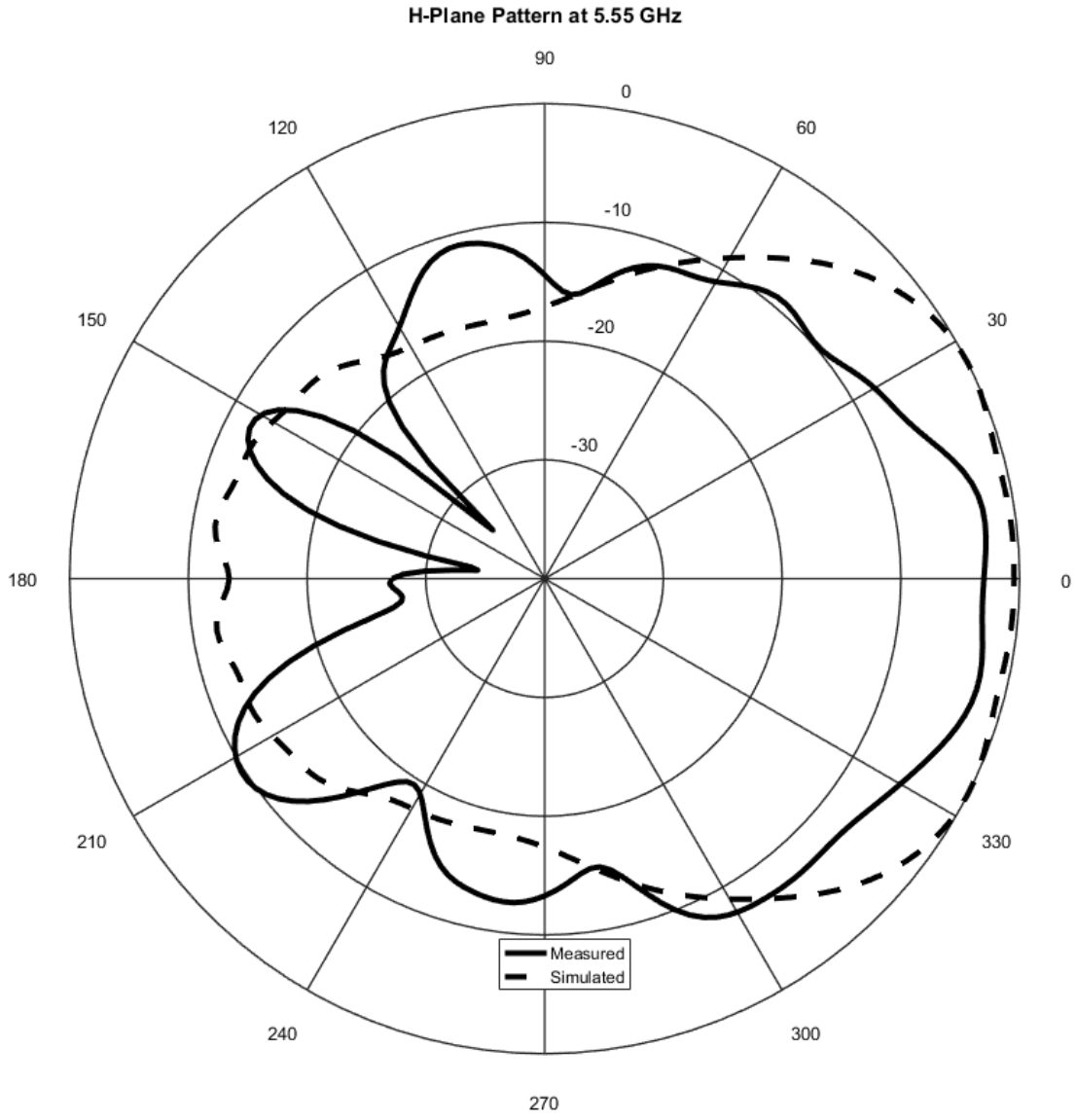

Fig. 4.7: H-Plane Radiation Pattern @5.55 GHz

4.6 Discussion

From Fig.4.3 it is clearly seen that the simulated and measured reflection coefficients matched well at the expected resonance frequency bands, However, there are some unexpected resonances in the measured reflection coefficient which was not observed in the simulation results. By analysing the reflection coefficient, it was suspected that the edges of the ground plane of the patch antenna and the copper reflector were short circuited in some

part during fabrication due to the foam nature of the substrate and created a cavity. Those unexpected resonances were due to the cavity resonance. To confirm this assumption, the edges of the fabricated antenna was covered with copper tape and the measurements were carried out again. The unexpected resonances observed from this measurement as well and it happened at the same frequency as before, which confirmed the assumption.

Table 4.2,Fig. 4.4, Fig. 4.5, Fig. 4.6, and in Fig. 4.7shows that the simulated and measured gain, E-plane and H-plane radiation patterns matches well, which confirmed the validness of this design. The next step is to inkjet print this antenna on the wing or other parts of UAV and characterize the antenna performance.

CHAPTER 5
SUMMARY AND FUTURE WORK

5.1 Summary

This thesis work reported a faster, better and cheaper way of inkjet printing antennas on the cover glass of the solar cells of the small spacecrafts or directly on their solar cells. This method also can be used to inkjet print conformal antennas on the wing or other parts of a UAV body.

To verify the effectiveness of this method, a series of printing experiments were carried out by inkjet printing some conformal antenna geometries such as sold patch antenna, meshed patch antenna and spiral antenna on a space certified AF32 glass substrate. The printed traces were examined using the fiducial camera built-in the Dimatix material printer. Furthermore, the inkjet printed antenanas were measured and found to be functional.

A high gain highly transparent reflectarray was inkjet printed on space certified glass substrates using the printing procedures outlined in this thesis. The reflectarray was measured with and without solar panels to verify antenna performance. Test results showed that the inkjet printed reflectarray on glass can provide at least 21.5 dB of gain. Solar panel measurements were also done to see how the reflectarray installed on top of the solar panel effects the solar panel efficiency. The test results were summarized and a brief discussion about the test results was given.

At the end, a conformal dual-band antenna for UAV application was designed and fabricated in the lab. The antenna was measured to verify its performance. The measurement results agreed well with the simulated results.

In summary, a faster, better and cheaper way of inkjet printing antennas on rigid flat surfaces such as glass was reported. This method was used to inkjet print several conformal antenna geometries on space certified glass substrates and the antenna performance was

characterized. A conformal dual-band antenna was designed and fabricated, the antenna was measured to verify its performance.

5.2 Future work

Inkjet printing is one of the promising fabrication techniques for future printed electronics due to its high resolution, low cost and easy of operation. The following future work could be done with the printing procedures developed in this thesis or by optimizing it according to the specific research needs.

(1) Inkjet printing on different types of substrates

Although this thesis work focused on inkjet printing of antennas on space certified glasses, the same printing procedures can be used to inkjet print antennas or microwave circuitry on any other flat flexible or rigid substrates. One of the interesting topic is to inkjet print antennas on Acrylics. Since acrylics offers higher transparency and less darkening effect for solar panel integration.

(2) Developing in-house ink

One of the drawbacks of the inkjet printing techniques is that the available inks on the market is limited and they can be used to print on a certain type of substrates. One way to overcome this issue is to develop in-house inks with specific properties to satisfy the inkjet printing needs. Since the Dimatix printer uses disposable cartridge and print-heads, it is worthwhile to developing custom inks with special characteristics such as biocompatible, low curing temperature etc.

(3) Design and inkjet print the conformal dual-band antenna on UAV body

It is very interesting to redesign the conformal dual-band antenna proposed in this thesis work using composite materials, which is used for UAV prototyping and inkjet print the designed antenna with the printing techniques developed in this thesis work.

REFERENCES

[1] [Online]. Available: https://www.nasa.gov/directorates/spacetech/small_spacecraft/smallsat_overview.html

[2] [Online]. Available: http://space.skyrocket.de/doc_sat/cubesat.htm

[3] [Online]. Available: http://www.nanosats.eu/index.html#figures

[4] T. W. Turpin and R. Baktur, "Meshed patch antennas integrated on solar cells," *IEEE Antennas and Wireless Propagation Letters*, vol. 8, pp. 693–696, 2009.

[5] S. Vaccaro, C. Pereira, J. Mosig, and P. De Maagt, "In-flight experiment for combined planar antennas and solar cells (solant)," *IET microwaves, antennas & propagation*, vol. 3, no. 8, pp. 1279–1287, 2009.

[6] S. Vaccaro, P. Torres, J. Mosig, A. Shah, J.-F. Zurcher, A. Skrivervik, F. Gardiol, P. De Maagt, and L. Gerlach, "Integrated solar panel antennas," *Electronics Letters*, vol. 36, no. 5, pp. 390–391, 2000.

[7] T. W. Turpin and R. Baktur, "Meshed patch antennas integrated on solar cells," *IEEE Antennas and Wireless Propagation Letters*, vol. 8, pp. 693–696, 2009.

[8] J. A. Arellano, "Inkjet-printed highly transparent solar cell antennas," Master's thesis, Utah State University, Logan, UT, 2011.

[9] M. Maimaiti, "Study of inkjet printing as an ultra-low-cost antenna prototyping method and its application to conformal wraparound antennas for sounding rocket sub-payload," Master's thesis, Utah State University, Logan, UT, 2013.

[10] L. Josefsson and P. Persson, *Conformal array antenna theory and design*. John wiley & sons, 2006, vol. 29.

[11] V. Subramanian, J. B. Chang, A. de la Fuente Vornbrock, D. C. Huang, L. Jagannathan, F. Liao, B. Mattis, S. Molesa, D. R. Redinger, D. Soltman *et al.*, "Printed electronics for low-cost electronic systems: Technology status and application development," in *Solid-State Device Research Conference, 2008. ESSDERC 2008. 38th European*. IEEE, 2008, pp. 17–24.

[12] A. Teichler, J. Perelaer, and U. S. Schubert, "Inkjet printing of organic electronics–comparison of deposition techniques and state-of-the-art developments," *Journal of Materials Chemistry C*, vol. 1, no. 10, pp. 1910–1925, 2013.

[13] Y. Kim, B. Lee, S. Yang, I. Byun, I. Jeong, and S. M. Cho, "Use of copper ink for fabricating conductive electrodes and rfid antenna tags by screen printing," *Current Applied Physics*, vol. 12, no. 2, pp. 473–478, 2012.

[14] H. Sirringhaus, T. Kawase, R. Friend, T. Shimoda, M. Inbasekaran, W. Wu, and E. Woo, "High-resolution inkjet printing of all-polymer transistor circuits," *Science*, vol. 290, no. 5499, pp. 2123–2126, 2000.

[15] H.-H. Lee, K.-S. Chou, and K.-C. Huang, "Inkjet printing of nanosized silver colloids," *Nanotechnology*, vol. 16, no. 10, p. 2436, 2005.

[16] T. Boland, T. Xu, B. Damon, and X. Cui, "Application of inkjet printing to tissue engineering," *Biotechnology journal*, vol. 1, no. 9, pp. 910–917, 2006.

[17] F. Hermerschmidt, P. Papagiorgis, A. Savva, C. Christodoulou, G. Itskos, and S. A. Choulis, "Inkjet printing processing conditions for bulk-heterojunction solar cells using two high-performing conjugated polymer donors," *Solar Energy Materials and Solar Cells*, vol. 130, pp. 474–480, 2014.

[18] M. Hilder, B. Winther-Jensen, and N. Clark, "Paper-based, printed zinc–air battery," *Journal of power Sources*, vol. 194, no. 2, pp. 1135–1141, 2009.

[19] S. H. Yu, B. J. Kim, M. S. Kang, S. H. Kim, J. H. Han, J. Y. Lee, and J. H. Cho, "In/ga-free, inkjet-printed charge transfer doping for solution-processed zno," *ACS applied materials & interfaces*, vol. 5, no. 19, pp. 9765–9769, 2013.

[20] E. Tekin, P. J. Smith, and U. S. Schubert, "Inkjet printing as a deposition and patterning tool for polymers and inorganic particles," *Soft Matter*, vol. 4, no. 4, pp. 703–713, 2008.

[21] J. R. Castrejon-Pita, W. Baxter, J. Morgan, S. Temple, G. Martin, and I. Hutchings, "Future, opportunities and challenges of inkjet technologies," *Atomization and sprays*, vol. 23, no. 6, 2013.

[22] H. Dong, W. W. Carr, and J. F. Morris, "An experimental study of drop-on-demand drop formation," *Physics of fluids*, vol. 18, no. 7, p. 072102, 2006.

[23] [Online]. Available: https://www.fujifilmusa.com

[24] [Online]. Available: http://www.schott.com

[25] [Online]. Available: http://www.microfab.com/complete-systems/jetlab-tabletop

[26] L. J. Millet, M. B. Collens, G. L. Perry, and R. Bashir, "Pattern analysis and spatial distribution of neurons in culture," *Integrative Biology*, vol. 3, no. 12, pp. 1167–1178, 2011.

[27] T. W. Turpin, "Meshed patch antennas integrated on solar cell-a feasibility study and optimization," Master's thesis, Utah State University, Logan, UT, 2009.

[28] S. Ma, F. Ribeiro, K. Powell, J. Lutian, C. Møller, T. Large, and J. Holbery, "Fabrication of novel transparent touch sensing device via drop-on-demand inkjet printing technique," *ACS applied materials & interfaces*, vol. 7, no. 39, pp. 21 628–21 633, 2015.

[29] O. Azucena, J. Kubby, D. Scarbrough, and C. Goldsmith, "Inkjet printing of passive microwave circuitry," in *Microwave Symposium Digest, 2008 IEEE MTT-S International*. IEEE, 2008, pp. 1075–1078.

[30] K. Black, J. Singh, D. Mehta, S. Sung, C. J. Sutcliffe, and P. R. Chalker, "Silver ink formulations for sinter-free printing of conductive films," *Scientific reports*, vol. 6, p. 20814, 2016.

[31] T. Yekan and R. Baktur, "An experimental study on the effect of commercial triple junction solar cells on patch antennas integrated on their cover glass," *Progress In Electromagnetics Research C*, vol. 63, pp. 131–142, 2016.

[32] D. Lewis, A. Martinez, and A. Petro, "Integrated solar array and reflectarray antenna for high bandwidth cubesats," 2015.

[33] T. Yekan, R. Baktur, C. Swenson, H. Shaw, and O. Kegege, "Integrated solar-panel antenna array for cubesats (isaac)," 2016.

[34] [Online]. Available: http://www.schott.com

[35] K. P. Valavanis and G. J. Vachtsevanos, *Handbook of unmanned aerial vehicles*. Springer Publishing Company, Incorporated, 2014.

[36] C. Zhang and J. M. Kovacs, "The application of small unmanned aerial systems for precision agriculture: a review," *Precision agriculture*, vol. 13, no. 6, pp. 693–712, 2012.

[37] I. Colomina and P. Molina, "Unmanned aerial systems for photogrammetry and remote sensing: A review," *ISPRS Journal of Photogrammetry and Remote Sensing*, vol. 92, pp. 79–97, 2014.

[38] I. Maza, F. Caballero, J. Capitán, J. R. Martínez-de Dios, and A. Ollero, "Experimental results in multi-uav coordination for disaster management and civil security applications," *Journal of intelligent & robotic systems*, vol. 61, no. 1, pp. 563–585, 2011.

[39] S. Maci, G. B. Gentili, P. Piazzesi, and C. Salvador, "Dual-band slot-loaded patch antenna," *IEE Proceedings-Microwaves, Antennas and Propagation*, vol. 142, no. 3, pp. 225–232, 1995.

[40] N. Behdad and K. Sarabandi, "Dual-band reconfigurable antenna with a very wide tunability range," *IEEE Transactions on Antennas and Propagation*, vol. 54, no. 2, pp. 409–416, 2006.

[41] [Online]. Available: http://www.rohacell.com